Dissertation zur Erlangung des Doktorgrades

der Fakultät für Chemie und Pharmazie

der Ludwig-Maximilians-Universität München

Decoy gelatin nanoparticles as a novel tool to elucidate the role of NF-κB in Kupffer cells on hepatic ischemia/reperfusion injury

Florian Hoffmann

aus München

2007

1 CONTENTS

2 INTRODUCTION

2.1 Background and aim of the study

The liver-resident Kupffer cells play an important role in inflammatory liver signalling. Exposure to pathogens like bacteria and viruses, as well as diverse hepatic disorders such as ischemia/reperfusion injury and alcoholic liver disease, lead to an activation of the redox-sensitive transcription factor Nuclear Factor κB (NF-κB). As a consequence, proinflammatory chemokines and cytokines like Tumor necrosis factor α (TNF-α) are produced and released. However, the effect of NF-κB in liver tissue is highly cell-type specific. Whereas exceeding NF-κB activation in Kupffer cells is associated with liver inflammation, NF-κB in hepatocytes acts in a protective manner by the transcription of antiapoptotic genes. A global inhibition of hepatic NF-κB, irrespective of the cell type targeted was shown to increase TNF-α mediated apoptosis (1), to impair liver regeneration after partial hepatectomy (2) and to enhance injury after hepatic ischemia/reperfusion (3). Consequently, a universal hepatic inhibition of NF-κB is not a therapeutic option, which makes the need for a selective targeting of NF-κB in Kupffer cells obvious.

Thus, the aim of this study can be outlined as follows:

1. Development of a specific carrier in order to deliver NF-κB binding decoy oligodeoxynucleotides selectively to the resident liver macrophages. To this end, solid gelatin nanoparticles were loaded with fluorescent NF-κB decoy oligodeoxynucleotides and the biodistribution was examined by confocal microscopy.

2. Providing the proof of principle for a selective NF-κB-targeting in Kupffer cells. Therefore, the influence of NF-κB decoy nanoparticles on lipopolysaccharide (LPS) challenged liver tissue in vivo was evaluated.

3. Investigation of the impact of a selective NF-κB inhibition in Kupffer cells on in vivo hepatic ischemia/reperfusion (IR) injury. For this purpose, the model of partial warm IR in rats was established in our group and decoy nanoparticles were administered before the induction of 70% liver ischemia, in order to compare the outcome to untreated animals.

2.2 Kupffer cells

The liver consists of both parenchymal (i.e. hepatocytes) and non-parenchymal cells (i.e. Kupffer cells, endothelial cells, and Ito or hepatic stellate cells). Hepatocytes account for up to 60% of liver cells and 90% of liver mass and are responsible for maintaining liver function, mainly metabolism, bile production and drug detoxification (4). Kupffer cells, contributing to 15% of liver cells and less than 3% of liver mass, are the largest population of resident macrophages in the body. Due to their strategic position within the liver sinusoids (Figure 1), Kupffer cells are the first macrophage cell type to come in contact with pathogens and microbial products, thus forming the primary line of host defense. They are actively phagocytic and represent an important cellular system for removal of particulate materials and microbes from the circulation. Their location just downstream from the portal vein allows Kupffer cells to efficiently scavenge bacteria that reach the blood flow of the portal veins through disruptions in the intestinal epithelium, thus preventing invasion of the systemic circulation. Rapidly after exposure to foreign bodies like viruses and bacteria, Kupffer cells produce and release a variety of proinflammatory cytokines and other agents necessary for the elimination of these pathogens (5;6), such as TNF-α, Interleukin (IL)-6, -12 and -1β, as well as nitrice oxide, reactive oxygen species (ROS) and chemokines like MIP-1 and -2 (6). Subsequently, microbicidal neutrophils are recruited to the activated Kupffer cells and immigrate rapidly in response to infection (7). Among these cytokines released, TNFα is one important member opposing the pathogenic threat. However, overexpression of TNFα leads to diminished hepatocyte viability and to increased liver damage (8;9).
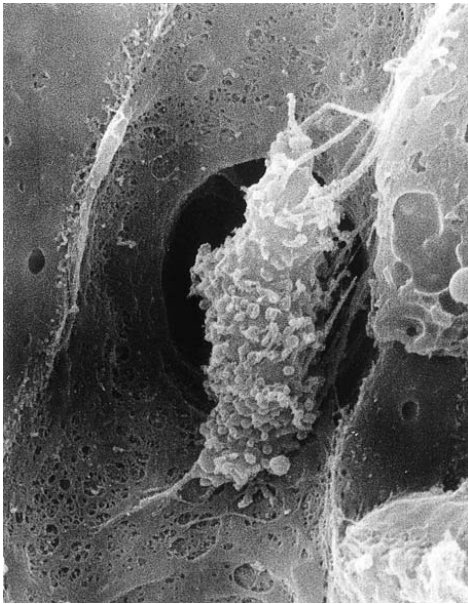
Figure 1   Localization of a Kupffer cell within the liver sinusoid (scanning electron microscopy image taken from Naito et al. (10)).

Kupffer cells play an important role in the pathogenesis of various liver diseases. During fibrosis, Kupffer cells release different cytokines like TGF-β_1, which in turn activates the hepatic stellate cells, the cell type mainly responsible for liver fibrosis (11). Alcohol-related liver disease is a chronic inflammatory disease of the liver parenchyma. Acute or chronic ethanol administration causes an increase in numbers of Kupffer cells and therefore brings about an enhanced production of inflammatory mediators such as IL-1, TNF-α and oxygen free radicals (11). In addition, ethanol ingestion seems to heighten the amount of gram negative bacteria in the bowel flora. Followed by a rise in the intestinal permeability, higher levels of LPS can be found in the portal vein, which subsequently activates the Kupffer cells (11).

Furthermore, Kupffer cell activity is found to be increased soon during postischemic reperfusion injury, which will be discussed in further detail below.

Moreover, Kupffer cells are important regulators for liver regeneration. The liver differs from the other interior organs due to its unique capability to restore its original mass, even after 70% of tissue extraction. Soon after resection, mediators like TNF-α and IL-6 are released by the liver macrophages, which primes hepatocytes to proliferate. The crucial role of Kupffer cells in this context is further

emphasized by the fact that depletion of the liver macrophages leads to diminished regeneration and proliferation (12).

Inhibition of Kupffer cell action can be achieved by different methods. Administration of the rare earth metal gadolinium (as gadolinium chloride) leads to Kupffer cell depletion within 24 hours, probably by exchange with Ca^{2+} ions and interaction with Ca^{2+} dependent processes. Liposomal encapsulated clodronate is taken up selectively by the liver macrophages and destroys Kupffer cells upon intracellular release. The fatty acid derivative methylpalmitate is thought to integrate into the cell membrane, which results in membrane breakdown. Furthermore, selective inhibition of Kupffer cell activity has been reported by the use of glycine (13).

Though Kupffer cell depletion has shown beneficial effects in various experimental inflammatory models (14;15), complete elimination of this important cell type from the liver is not a therapeutic option, since Kupffer cells are indispensable for intact immune function (16). In addition, several side effects like toxicity of gadolinium chloride on hepatocytes limit the use of Kupffer cell depleting agents.

2.3 NF-κB

2.3.1 General aspects

The redox-sensitive transcription factor NF-κB displays pleiotropic effects during inflammation, immune response, cell survival and proliferation (17).

Five members of the mammalian NF-κB family have been described so far – p50, p52, p65/RelA, p68/RelB, and p75/c-Rel (18-20). Inactive NF-κB is sequestered in the cytoplasm, where it is bound to its inhibitory protein IκB, which prevents translocation to the nucleus. Upon stimulation, like endotoxemia and TNF-α challenge, the upstream kinase IκB kinase (IKK) is phosphorylated (Figure 2), which in turn facilitates phosphorylation of the inhibitory protein IκB associated with NF-κB. After degradation of IκB by the 26S-proteasome, NF-κB is released from its cytoplasmic retention and translocates to the nucleus (20-22). In the nucleus, several

costimulating processes like acetylation by histone acetyltransferases (HAT) and phosphorylation are needed to enable NF-κB transcriptional activity.
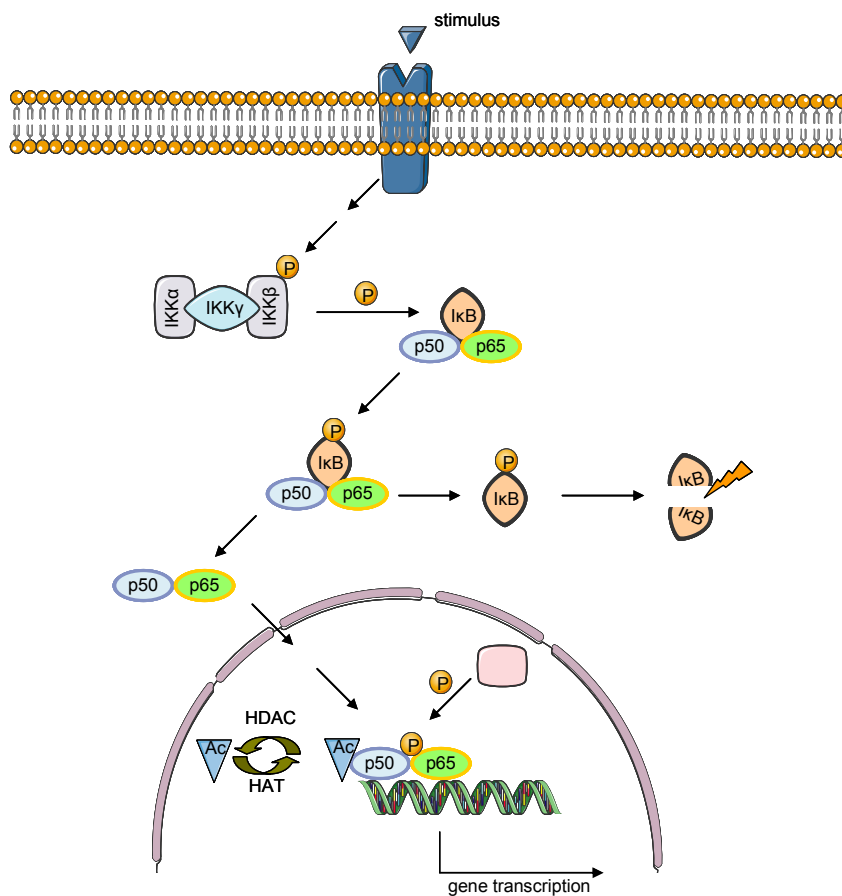
Figure 2   Classical pathway of NF-κB induction

However, other activation cascades of NF-κB occur as well. An alternative pathway is exclusively triggered by IKKα homodimers which results in a selective activation of p52/RelB heterodimers (23). Furthermore, in ischemia and reperfusion, the heterodimer p50/p65 translocates to the nucleus without previous ubiquitination and degradation of IκB (24). In summary, increasing evidence emerged that induction of NF-κB transcriptional activity is regulated at multiple levels, depending on the stimulus investigated.

NF-κB is mainly involved in B and T cell development under physiological conditions (25) and is a central mediator of the mammalian immune response. Many stimuli can rapidly activate NF-κB leading to the expression of various genes, basically cytokines, chemokines, cell adhesion molecules, stress response genes, growth factors and antiapoptotic regulators (20). NF-κB activity is upregulated in

many pathological conditions. As a key regulator of cytokine expression, NF-κB induction is a central event in inflammatory processes. Therefore it is not surprising to find NF-κB levels elevated in incidents like artherosclerosis, allergy and heart diseases (25).

The cytokine TNF-α is a prominent member of NF-κB target genes. Being a necessary mediator for immune host defense, TNF-α is involved in most NF-κB regulated responses. However, exceeding release of TNF-α is linked to excessive inflammation and cell damage. In addition, TNF-α itself stimulates NF-κB translocation, creating a positive feed-back loop. Therefore, duration and dimension of TNF-α secretion is a decisive factor for the extent of inflammation (26).

2.3.2 NF-κB in the liver

The role of NF-κB in liver tissue is highly cell-type specific (Figure 3). Activation of NF-κB in the resident liver macrophages upon inflammatory stimuli causes increased expression of proinflammatory cytokines, which leads to inflammation and liver failure (27;28). Kupffer cells are thought to be the main source of TNF-α in the liver, and TNF-α gene transcription is strongly regulated by NF-κB (29). This predestines NF-κB as a promising target for antiinflammatory therapy. Induction of NF-κB activity in hepatocytes however is linked to cellular protection by increasing the transcription of antiapoptotic genes (30). Therefore, a systemic inhibition of NF-κB in the liver for suppression of hepatic inflammation is not feasible, as this results in increased hepatocyte apoptosis (1). The dual role of NF-κB in the liver is further underlined by the fact that p65 knock-out mice die during embryogenesis due to massive hepatocyte apoptosis (31).

NF-κB is also an essential factor for liver regeneration. After partial liver resection, NF-κB is activated in Kupffer cells as well as in hepatocytes, thus triggering cell proliferation. An increase of liver macrophage NF-κB effects a release of mitogens like IL-6 (32), which in turn acitvates NF-κB in heptocytes (33). Subsequently, hepatocytes enter the cell cycle. Selective inhibition of NF-κB in hepatocytes entails

increased apoptosis and diminished proliferation after partial hepatectomy (34), and inhibition of NF-κB in Kupffer cells reduces liver regeneration capacity as well (2).
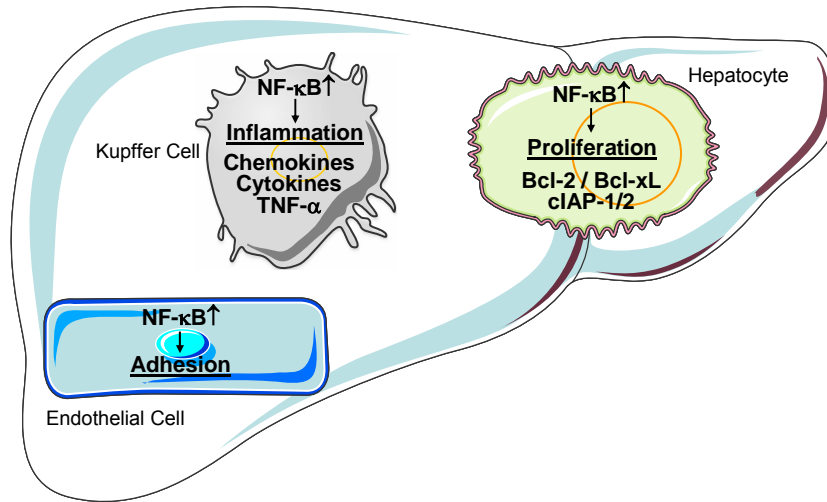
Figure 3   Cell-type dependent effects of NF-κB activation

In the light of the beneficial and antiapoptotic properties of NF-κB in hepatocytes, the requirement for a Kupffer cell selective inhibition of NF-κB is obvious (8;35).

2.3.3 NF-κB inhibitors

There is currently an abundance of more or less specific NF-κB inhibitors available, interacting with the NF-κB activation cascade at numerous sites (36;37). Being a redox-sensitive transcription factor, a multitude of antioxidants is utilized, in particular gluthation, N-acteyl-cysteine (NAC) and pyrrolidinedithiocarbamate (PDTC). Several medicinal drugs like aspirine, ibuprofen and sulfasalazine inhibit phosphorylation of the inhibitory protein IκBα, thus preventing its displacement from the cytoplasmatically retained NF-κB. As IκBα is degraded by ubiquitination, proteasome inhibitors like cyclosporin and tacrolimus inhibit NF-κB translocation as well. Other inhibitors act at the nuclear stage, for instance by hindering nuclear transport (leptomycin B) or by interacting with acetylation processes of NF-κB

(glucocorticoids). However, an interaction of these molecules with other targets and therefore various side effects by their use can not be ruled out.

IκB as the regulatory switch displays a logical target for inhibition, and overexpression of IκB (38) has been tested. But these approaches are time-consuming and safety issues remain a key problem.

There are at least four different IKK inhibitors currently in clinical trials. As an important upstream activator of NF-κB signalling, interference with the IKK-cascade seems a promising approach for anti-inflammatory treatment. However, long-term studies are still missing and especially side effects like teratogenicity and susceptibility to infections could present major limitations for the therapeutic use (39). Moreover, recent studies revealed that hepatocyte-specific deletion of the NEMO-subunit caused hepatocellular carcinoma in 12 month old mice (40). Although all tested IKK-inhibitors basically target IKK2, further investigations will be needed to rule out any cross-reactions.

Thus, there is still a need for the development of more specific NF-κB inhibitors with less occurring side effects.

2.4 Decoy oligodeoxynucleotides

A more suitable tool for interacting with transcription factors like NF-κB is the double-stranded NF-κB decoy oligodeoxynucleotides (ODNs) corresponding to the promoter sequence, as imprecise interactions are less likely to occur due to the specific binding of the transcription factor to decoy oligonucleotides.

A transcription factor translocates to the nucleus after stimulation and activation, where it binds to the so called promoter region of its particular gene. The promoter region contains the consensus sequence, a highly specific order of base pairs that is recognized by the transcription factor. The subunits p50 and p65 for instance associate to a five (GGGAC) and a four (TTCC) base-pair consensus-sequence, respectively.

Transfection of double-stranded oligonucleotides leads to competitive cis-trans interactions between oligonucleotides and the transcription factor, thus preventing binding of the transcription factor to the designated genomic DNA (41). The cell is actually flooded with these short DNA-strands, and the transcription factor can not distinguish between the artificial binding sites in the cytoplasm and the original locus in the nucleus. The advantage of using decoy oligonucleotides lies in the specificity of the binding and therefore in the mode of inhibition. As the consensus-sequence is only recognized by the predestined transcription factor, unwanted side effects can be ruled out.
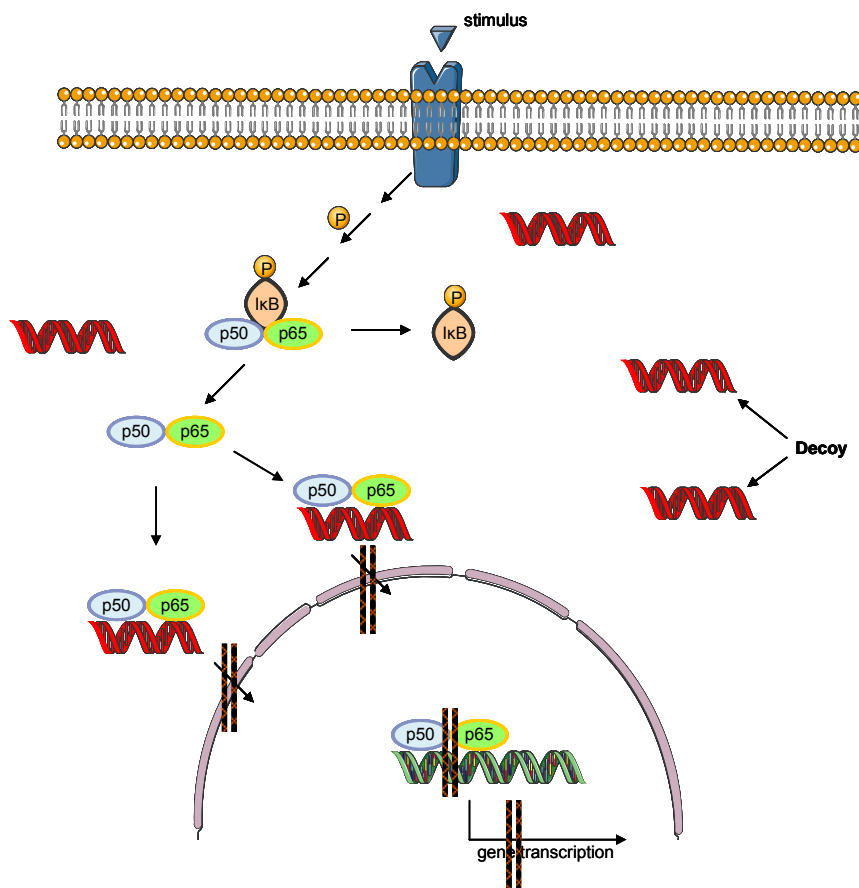
Figure 4   Model of decoy-transcription factor interaction

The utilization of NF-κB decoys (42;43) has been shown to have beneficial effects in the models of renal ischemia/reperfusion injury (44), hepatic metastasis of murine reticulosarcoma (45) and neuronal damage after brain ischemia (46).

2.5 Carriers

Under physiological conditions, decoy oligonucleotides are negatively loaded. Hence, a passage through the lipophilic cell membrane is almost impossible. Transfection of oligonucleotides into cells takes place only at very low transfection rates. Therefore, a potent carrier has to be used to transport the decoys to the target cells. As binding of decoy oligonucleotides to the transcription factor occurs in a dose-dependent manner, sufficient delivery to the cytoplasm is of utmost importance.

2.5.1 Targeting of Kupffer cells

Kupffer cells are the largest resident macrophage population in the body and are located within the liver sinusoids. Thus, they come in contact with every particle in the hepatic blood circulation. As Kupffer cells have a high phagocytic activity, many carriers are taken up by these macrophages, and numerous studies were conducted on avoiding Kupffer cell incorporation. However, for an exclusive targeting of Kupffer cells without affecting other cell types in vivo, a modification of carriers for specific delivery is necessary.

Kupffer cells possess sugar derivatives recognizing receptors on the outside membrane. Hence, carriers provided with mannose and fucose residues on their surface are reported to be taken up at higher rates (47). This is basically practiced in conjunction with liposomal carriers. Liposomes are vesicular colloid particles composed of self-assembled amphiphilic molecules (48). Molecules to be delivered can be encapsulated into the interior or bound on the surface of the liposomes, which are taken up by cells either by endocytosis or by fusion of the lipophilic cell membranes with the liposomal outside layer (49). Incorporation of the hemagglutinating virus of Japan (HVJ) components into liposomes results in further enhanced Kupffer cell uptake. However, mode of administration in this context seems to be of great importance, as application by intravenous injection causes lower Kupffer cell transfection than direct intraportal infusion (50).

Moreover, coupling of substances to low-density lipoprotein (51) and to serum albumin (52) are additional alternatives for Kupffer cell targeting, but a noticeable portion of applied material is transported to endothelial cells as well.

Adenoviral gene transfer is often used as vector for gene delivery. However, administration of an adenoviral vector resulted in an higher inflammatory response of Kupffer cells (53), an effect that has been reported to a lower extent for nanoparticulate carriers as well (54).

2.5.2 Carriers for oligonucleotides

Oligonucleotides used as decoys or as antisense nucleotides are useful tools for interacting with cellular processes. Nevertheless, selective delivery of oligonucleotides remains a key problem, and the search for carriers that fulfill this requirement has been intensified. Liposomes and nanoparticles have emerged as the most suited ones for the delivery of oligonucleotides. Both lie within in the same size range from 10 to 1,000 nm and belong to the colloidal dispers systems. Fluid-type liposomes have turned up as the state-of-the-art carrier for the delivery of oligonucleotides (49), as they provide for easy and sufficient delivery of incorporated oligonucleotides to cells. However, directed targeting of liposomes to certain cell types is not possible without deeper modifications, because liposomes tend to fuse with all kinds of cells. Nanoparticles have to be taken up by endocytosis, which leaves phagocytic competent cells as main targets. Upon intravenous administration, nanoparticles are rapidly cleared from the circulation through phagocytosis, preferentially by macrophages of the reticuloendothelial system (RES) concentrating mainly in liver and spleen (55). Nanoparticles can be manufactured from biodegradable polymers, for example polylactic acid, polyglycolic acid and chitosan (56), and they have been shown to be more efficient drug carriers than liposomes due to their better stability and lower toxicity (57).

The oligonucleotides are either covalently or reversibly bound to the nanoparticle surface. After endocytosis, oligonucleotides have to be released from the lysosomal

compartment, which can present a major limitation for exerting a biological effect (57).

2.5.3 Gelatin nanoparticles

A pronounced uptake into Kupffer cells of surface-modified liposomes has been described (47;49;50), but also a relevant delivery to hepatocytes could not be eliminated (58). Therefore, a tool for the selective targeting of Kupffer cells with oligonucleotides has not been developed so far. This prompted us to evaluate if a nanoparticulate carrier composed of gelatin can be used for the delivery of NF-κB decoy oligonucleotides to Kupffer cells. Solid nanoparticles display advantages over the use of liposomes because of their higher stability, lower toxicity and better efficiency in drug delivery (57).

Gelatin is a well known biodegradable protein with low immunogenic properties and displays a safe and non-toxic material, as it is widely used in medicine as ingredient in various plasma expanders. It is a natural macromolecule that can be easily obtained by heat dissolution and partial hydrolysis of collagen in animal skins, bones and tendons.

Nanoparticles made from gelatin were first described in 1978 (59) and their manufacture has been improved steadily ever since (60). They offer the advantages of a simple and safe delivery system, and nanoparticles consisting of a solid gelatin core have been proven to be a well suited carrier system for double stranded oligonucleotides. By introducing positive charges on the surface of the gelatin nanoparticles, negatively charged nucleotides can be stably loaded onto the particles due to ionic interactions (61;62). Unmodified gelatin nanoparticles have already been reported to be taken up by dendritic cells (63) and B16 F10 mouse melanoma cells (62) in vitro.

The exact manufacturing protocol and characteristic properties of the nanoparticles used in this study are described by Jan Zillies in his PhD thesis from 2007.

2.6 LPS

The glycolipid lipopolysaccharide (LPS) is a component of the outer membrane of gram-negative bacteria and has the ability to evoke a strong inflammatory response. The liver is a final barrier that hinders gut-derived LPS from entering the circulation, thus playing an important role in clearing LPS from the systemic blood stream (64).

Upon contact of the endotoxin with a LPS-recognition receptor expressed on the cell-surface, the so called Toll-like receptor (TLR) 4, an intracellular cascade is initiated. With the participation of various cofactors, the IKK-activity is ultimately induced, which leads directly to an activation of NF-κB (17;64).

After systemic LPS challenge, the mRNA expression of various cyokines like TNF-α are soon upregulated, and the rise in mRNA levels correlates with the status of NF-κB activation. Inhibition of NF-κB by PDTC for instance, abolished LPS induced cytokine and chemokine expression (65).

Due to their location in the liver sinusoids, Kupffer cells are among the first cell types to be exposed to LPS from the intestine. This fact, in addition to their high phagocytic activity makes them the most important scavenger for circulating endotoxin. Depletion of Kupffer cells with gadolinium chloride lead to an increased survival with diminished cytokine release (66), pointing to the significance of the resident liver macrophages in LPS clearance.

Kupffer cells are the most prominent members of the liver cell population to generate TNF-α. Stimulation of isolated hepatocytes with LPS is not able to provoke a release of TNF-α, unless a co-culture model together with Kupffer cells is employed (67). Hepatocytes alone are not susceptible to LPS triggered apoptosis, but adding the supernatant of LPS-challenged Kupffer cells to the hepatocyte cell culture enhances liver cell death (68). Due to this relevance of Kupffer cells in mediating LPS induced TNF-α release, NF-κB as central modulator of TNF-α gene transcription in Kupffer cells becomes an apparent target for intervention.

The groups of Ogushi and Higuchi respectively (69;70) addressed this issue and used modified liposomal carriers (hemagglutinating virus of Japan (HVJ-) liposomes as

well as mannosylated cationic liposomes) to transfect Kupffer cells with NF-κB decoy oligonucleotides. Indeed, NF-κB-inhibition in LPS-treated mice showed a positive effect on cytokine expression and mouse survival. However, liposomal carriers are not an appropriate tool for targeting Kupffer cells alone, as other liver cells are affected as well.

2.7 Hepatic ischemia/reperfusion injury

2.7.1 General mechanisms

Ischemia/reperfusion (IR) injury is still a major cause for problems during liver transplantation and resection and accounts for up to 20% of liver transplant failures. There are two different models of hepatic IR in vivo, which are distinguished by the way of storage during the ischemic period. Warm IR (also named Pringle manoeuvre) is often used in clinical situations when surgical intervention on hepatic tissue is needed to prevent excessive bleeding, like liver resection. Warm IR is characterized by an overbalance of hepatocyte damage to non-parenchymal cell injury (71). Cold IR occurs mainly during transplantation procedures, as the harvested organ has to be delivered to the recipient. This transportation period can last for up to several hours, and to ensure the best possible organ quality, the liver is stored at 4°C in the so called University of Wisconsin (UW) solution.

While the manifestation of the actual damage is thought to occur with the onset of reperfusion, the basic deterioration begins during the ischemic period, and prolonged ischemia times correlate with poorer outcome of organ preservation. Soon after disconnection from the blood stream, the loss of mitochondrial respiration due to the lack of oxygen leads to ATP depletion and a subsequent deterioration of energy-dependent pathways (72). Thereupon, anaerobic processes lead to a shift of cellular pH towards acidosis (73). To reduce the metabolic rates, which enables anoxic cells to maintain essential metabolic functions for a longer time period, organs for liver transplantations are initially cooled down and kept on ice for transportation. During

warm ischemia, where the organ is held at normal body temperature, a further important stimulus for organ damage during the ischemic period is given by the increased activities of non-lysosomal proteases (72).

The amplification of liver damage in the reperfusion period can be divided into two distinct phases, an immediate (or acute) and a late (subacute) phase. The initial period (<2 h after reperfusion) is characterized by oxidant stress. The late phase of liver injury from 6 to 48 h after hepatic reperfusion is an inflammatory response mediated by infiltrating neutrophils (73).
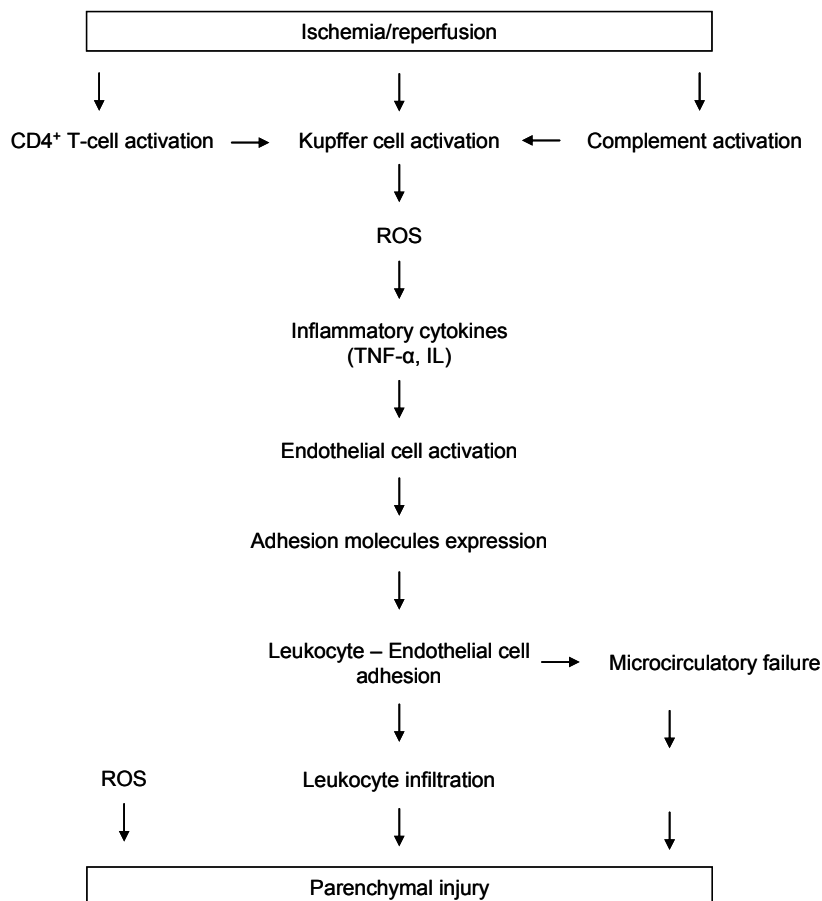
Figure 5   Schematic illustration of the pathophysiology of liver ischemia/reperfusion injury

After initiation of reperfusion the liver is overwhelmed by the large amount of oxygen. Due to their strategic position in the liver sinusoids, Kupffer cells react fast after the sudden onset of blood and therefore oxygen supply (Figure 5). Reactive oxygen species (ROS) are considered to be produced by Kupffer cells within few

minutes, which subsequently triggers production and release of a plethora of cytokines like TNF-α and IL-1 (74). Moreover, ROS can have direct cytotoxic effects on hepatocytes. The released cytokines induce endothelial cells to express adhesion molecules like Intercellular Adhesion Molecule (ICAM)-1 and E-selectin on their cell surface. This marks the beginning of the late phase of IR injury, which is characterized by the interaction of endothelial cell adhesion molecules with their counterparts on circulating neutrophils (74). In addition, release of chemokines like cytokine-induced neutrophil chemoattractant (CINC) and macrophage inflammatory proteins (MIP)-1 and-2 contribute to neutrophil recruitment to the injured tissue. After contact of neutrophils with endothelial cells and aggravation of adhesion, the recruited neutrophils begin to extravasate to the parenchyma. Adherence to hepatocytes finally leads to degranulation, subsequent protease release and a long-lasting oxidant stress, resulting in parenchymal injury. In addition, neutrophils attached to endothelial cells form an obstacle within the sinusoids, which is associated with a decline in blood flow and therefore microcirculatory failure (75).

The radical NO is synthesized by the enzyme NO synthetase (NOS). There exist two isoforms of NOS in the liver, endothelial NOS (eNOS) and inducible NOS (iNOS). The role of NO formation during IR is very controversial. NO radicals can be converted to peroxynitrite by reaction with the ROS superoxide. Peroxynitrite itself is cytotoxic by exerting different effects, e.g. lipid peroxidation. Therefore, inhibition of NO formation should ameliorate hepatic IR injury. On the other hand, NO is necessary for maintaining liver blood flow. Several studies have been conducted for elucidating the role of NO in IR injury. However, detrimental as well as beneficial effects of NO have been reported, which is thoroughly discussed by Jaeschke (74).

Many insights into the role of Kupffer cells for ischemia/reperfusion injury were obtained through studies with depleted Kupffer cells. As described in chapter 2.2 various methods for eliminating the resident liver macrophages exist. Depletion of Kupffer cells has been shown to ameliorate warm hepatic ischemia/reperfusion injury, as demonstrated by reduction of transaminase levels (76), diminished CINC release and neutrophil infiltration (77), reduced TNF-α plasma levels (78) and by increased survival after 1 hour of total hepatic ischemia (79). However, Kupffer cells

seem to be indispensable for liver regeneration, as their elimination delays liver regeneration (80) and decreases the survival rate after partial hepatectomy (81).

In summary, Kupffer cells possess a key role in the signalling events leading to ischemia/reperfusion injury, but are also essential for liver regeneration.

2.7.2 Role of NF-κB

ROS play a crucial role in the initial period of postischemic reperfusion injury. Hence, being a redox-sensitive transcription factor, hepatic NF-κB levels are increased soon after the beginning of the reperfusion period (82;83). However, evidence emerged that the NF-κB activation cascade is likely to be triggered differently in hepatic ischemia/reperfusion (24). Phosphorylation of IκBα is normally executed on serines 32 and 36, for instance after TNF-α or LPS challenge. In the context of liver IR, IκBα is only phosphorylated on tyrosine 42. Fan et al (84) postulate that this activation scheme is occurring independently from the IKK-complex, but rather relies on c-Src mediated phosphorylation. Consequently, IκBα is not targeted for ubiquitin mediated degradation by the proteasome, thus remaining undisrupted in the cytoplasm.

The relevance of NF-κB in this context can be estimated by the fact, that suppression of NF-κB by antioxidants (85), radical scavengers (86) or NF-κB inhibitors (87) in fact decreased TNF-α release, transaminase levels and liver damage. Inactivation of NF-κB enhancing pathways, for instance by deletion of the upstream kinase IKK2 (88) or by overexpression of inhibitory IκBα (38), abrogated IR induced increase in hepatocellular injury. However, as described in section 2.3.2, the dual role of NF-κB applies to the setting of hepatic ischemia/reperfusion as well. So it is not surprising to find reports indicating rather a protective role for NF-κB in liver IR (89;90). Recently, Lentsch and colleagues (91) were able to show that higher NF-κB levels in hepatocytes during IR are linked with protection, while an increase of NF-κB in Kupffer cells rather induces TNF-α release and liver damage. However, their studies were based on isolated parenchymal and non-parenchymal cells from livers that had experienced warm ischemia/reperfusion. An in vivo evaluation of this issue was not

possible so far due to a missing possibility for selective interference with NF-κB in Kupffer cells.

2.7.3 Interventions

Several approaches for improving the injury caused by postischemic reperfusion have been investigated. The following sections will just provide a short overview, as a detailed listing would go beyond the scope of this work.

As production and release of ROS are central events in IR injury, many antioxidative interventions were tried, like thiol-containing compounds (as N-acteylcysteine or gluthathione), oxygen radicals scavenging enzymes (superoxide dismutase, catalase), lipoic acid and allopurinol (92). All these compounds have been reported to be efficacious in the treatment of reperfusion injury, but to date none of these strategies have found the way into routine clinical practice (93).

Further pharmacological interventions include a plethora of molecules. Hormone preconditioning with the atrial natriuretic protein (ANP) produced positive results (94), as did the use of pentoxyfilline (as an inhibitor of TNF-α synthesis), cyclosporine (inhibition of neutrophil infiltration) and adenosine agonists (93).

The most commonly used buffer for organ preservation is the University of Wisonsin (UW) solution. Storage of harvested livers in UW solution results in minimized cell swelling, inhibited ROS production and increased adenosine triphosphate repletion. Several studies have tried to specify the active ingredients. Apparently, the beneficial effects of the UW solution are provoked by the mixture of different compounds, as single components are not able to exert similar results (95).

Today, the only powerful strategy used in clinical practice is ischemic preconditioning (IP), consisting of a brief period of ischemia followed by a short interval of reperfusion before the actual surgical procedure. Ischemic preconditioning is connected with increased organ survival and diminished tissue damage. The method of IP is easily applicable in clinical situations, which makes this intervention very attractive. The mechanisms leading to the amelioration of reperfusion injury

were thoroughly investigated, and many targets have been named like adenosine, heat shock proteins and nitric oxide (96). The controversy about NF-κB in the liver during IP continues. While some reports indicate that NF-κB levels in the postischemic reperfusion period are diminished (97), an increase in NF-κB activity was also detected (98), which emphasises the contradictory and still unsettled role of NF-κB in the liver. Despite the growing number of reports investigating the mechanisms of hepatic protection by ischemic preconditioning, the present understanding of the ongoing processes is still of preliminary character (99).

Generally it can be said that preconditioning with apparently damaging interventions like TNF-α seem to ameliorate reperfusion injury (100).

Numerous interventions to improve the aftermath of postischemic liver damage have been subject of intensive research. However, not many interventions have found their way into everyday clinical situations, as the underlying mechanisms are still poorly understood.

The transcription factor NF-κB might present a promising target for the treatment of hepatic ischemia/reperfusion injury. However, before using NF-κB inhibitors as drugs to prevent IR caused damage, the dual role of NF-κB in this context has to be evaluated in more detail. Hence, our aim was to utilize decoy nanoparticles as a tool for a selective downregulation of NF-κB in Kupffer cells, to clarify the function of this transcription factor in this liver cell type.

3 MATERIALS AND METHODS

3.1 Materials and solutions

Table 1   Materials

Product	Company
Lipopolysaccaride (E.coli serotype 055:B05)	Sigma-Aldrich, Taufkirchen, Germany
Bovine serum albumin (BSA)	Sigma-Aldrich, Taufkirchen, Germany

PBS	pH 7.4
123.2 mM	NaCl
3.16 mM	KH_2PO_4
10.4 mM	Na_2HPO_4
	H_2O

3.2 Decoy oligodeoxynucleotides

NF-κB decoy oligodeoxynucleotides (5'- AGT TGA G<u>GG GAC</u> T<u>TT CCC</u> AGG C -3', 5'- GCC TGG GAA AGT CCC CTC AAC T -3') and scrambled NF-κB decoy ODNs (5'- CCT TGT ACC ATT GTT AGC C -3', 5'- GGC TAA CAA TGG TAC AAG G -3') were obtained from Biomers, Ulm (biomers.net). Consensus sequences for p50 and p65 are underlined. For improved stability all ODNs were bridged with a phosphorothioate (PTO) backbone (57). Sequences for NF-κB decoy ODNs and scrambled decoy ODNs have been used elsewhere (101;102). For biodistribution studies cis-decoy ODNs were 5`-end-labeled with an Alexa Fluor® 488.

3.3 Gelatin nanoparticles

Preparation and loading of gelatin nanoparticles was done by Jan Zillies (Pharmaceutical Technology, Department of Pharmacy, University of Munich) and is described in more detail in his PhD thesis (2007).

3.3.1 Materials

Table 2   Materials used for gelatin nanoparticles preparation

Product	Company
Acetone	VWR, Ismaning, Germany
Cholaminechloridehydrochloride	Sigma-Aldrich Taufkirchen, Germany
EDC	Sigma-Aldrich, Taufkirchen, Germany
Gelatin type A	Sigma-Aldrich, Taufkirchen, Germany
Glutaraldehyde	Sigma-Aldrich, Taufkirchen, Germany
HCl	VWR, Ismaning, Germany
Texas Red® sulfonyl chloride	Invitrogen, Karlsruhe, Germany
(scrambled) decoy oligonucleotides	Biomers.net, Ulm, Germany
Alexa Fluor® 488 end-labeled decoy oligonucleotides (NF-κB decoy ODN$_{488}$)	Biomers.net, Ulm, Germany

3.3.2 Manufacture of decoy nanoparticles

Gelatin nanoparticles were prepared by the two-step desolvation method as described previously (60). In brief, 1.25 g gelatin was dissolved in water (5% [w/w]) under stirring (500 rpm) and heating up to 50°C. The resulting solution was fractionated in a first desolvation step by quickly adding 25 ml of acetone. The remaining sediment was dissolved in 25 ml of water. Nanoparticles emerged in a second desolvation step

by dropwise adding 50 ml of acetone. After 5 min of stirring, the in situ formed particles were stabilized by crosslinking with 43.8 µg glutaraldehyde. The concentration of the nanoparticle dispersions was determined gravimetrically after purification by centrifugation and redispersion.

Surface modification (cationization) of gelatin nanoparticles was performed with the quaternary amine cholamine in a modified procedure based on the method previously described by Coester (103): after preparation and purification, the nanoparticles were suspended in highly purified water and 50 mg cholamine were dissolved in the suspension. 50 mg EDC were added to the reaction vessel under constant stirring and the reaction was stopped after 3 h.

Aqueous nanoparticle dispersions containing 0.85 mg or 0.73 mg surface modified gelatin nanoparticles were incubated with 120 µl aqueous oligonucleotide solution containing 6 nmol NF-κB decoy ODN or 6 nmol scr decoy ODN respectively (i.e., 10% [w/w] drug loading) in a total volume of 1,200 µl highly purified water. For liver distribution studies equivalent amounts of fluorescent-labeled NF-κB decoy ODN_{488} were loaded onto the gelatin nanoparticles. Afterwards, sucrose was added in an excipient to oligonucleotide mass ratio of 200. The suspensions were freeze-dried in an EPSILON 2- 6D pilot scale freeze dryer from Martin Christ Freeze Dryers GmbH, Osterode, Germany. Rehydration was conducted directly before use in 169.8 µl and 146.3 µl respectively of highly purified water (leading to a concentration of 10% sucrose [w/v], which was almost isoosmotic) under adding a Tween® 80 solution (100 µg/µl) in a 1:1 ratio to the mass of gelatin nanoparticles. Finally, samples were completed with a 10% [w/v] sucrose solution to a total volume of 300 µl. Four samples were combined per animal study. Unloaded gelatin nanoparticles were accordingly treated.

Size and zetapotential of the applied gelatin nanoparticle batches were determined by dynamic light scattering (DLS) using a Zetasizer 3000 HSA (Malvern Instruments, Worcestershire, UK). Zetapotential measurements were conducted under standardized ionic conditions in 10 mM NaCl at pH 7.0.

3.3.3 Preparation of fluorescent cationic gelatin nanoparticles

Fluorescent labeled gelatin nanoparticles were prepared by covalent coupling of the gelatin base material with an amino reactive fluorescent dye. After the first desolvation step the remaining gelatine sediment was dissolved in 25 ml of water under constant stirring (500 U/min) and heating up to 50°C. 1 mg of the fluorescent dye (Texas Red®) was added to this solution after dissolving in acetone and the mixture was constantly stirred for 1 h (500 U/min) at 50°C. After this incubation period the regular gelatin nanoparticle manufacturing process was continued with the second desolvation step. Subsequent to purification, cationization was conducted as usual (see chapter 3.3.2).

3.4 DOTAP/DOPC liposomes

Drug loaded liposomes were prepared by ethanol injection with the oligonucleotide already present in the water phase. The chosen ODN lipid ratio is geared to the work of Ogushi who applied an NF-κB decoy oligonucleotide in a fatal liver failure murine model (69). 28.74 µl lipid ethanol stock solution (1.8 g DOTAP-Cl and 1.7 g DOPC in 10.0 g EtOH), were dropwise added into 1.5 ml aqueous oligonucleotide solution containing 15 nmol Alexa Fluor® 488 end-labeled NF-κB decoy ODN (i.e., 2% [w/w] drug loading) under constant stirring. The mixture was then 10x passed through a 0.22 µm sterile filter. This leads to a final volume of around 1.2 ml containing 12 nmol/ml NF-κB decoy ODN applicable for animal studies, equivalent to the sample volume of gelatin nanoparticle formulations.

3.5 Cell culture

3.5.1 Materials

Table 3   Materials and solutions used for cell culture

Product	Company
Collagenase H	Roche Diagnostics,Mannheim, Germany
Dulbecco`s modified eagle medium (DMEM) pH 7.0 – 7.5	Cambrex Profarmaco, Landen, Belgium
Fetal bovine serum (FBS)	PAA Laboratories, Linz, Austria
Neutral buffered formalin solution 10%	Sigma-Aldrich, Taufkirchen, Germany
L-Glutamine solution 200 mM	Cambrex Profarmaco, Landen, Belgium
Penicillin/Streptomycin (Pen/Strep) solution	PAA Laboratories, Linz, Austria
Trypsin solution	PAA Laboratories, Linz, Austria
Cell culture materials	PESKE, Aindling-Pichl, Germany
RAW 264.7 cell line	American Type Culture Collection (ATCC), Rockville, USA

Rinsing buffer	pH 7.35
115 mM	NaCl
25 mM	$NaHCO_3$
5.9 mM	KCl
1.18 mM	$MgCl_2$
1.23 mM	NaH_2PO_4
1.2 mM	Na_2SO_4
2.5 mM	$CaCl_2$
20 mM	Hepes
	H_2O

3.5.2 Culture of RAW-Macrophages

The murine macrophage cell line RAW 264.7 was cultivated in DMEM containing 10% FBS and 1% Glutamin. The cells grew in an adherent monolayer in polystyrole flasks in an area of 75 or 150 cm^2 and were passaged once or twice per week. For investigations, the cells were diluted and 3 x 10^6 cells/ 2 ml were seeded into a 6 well plate und cultivated for 3 days until the experiment.

Determination of cell concentration and viability was performed in Vi-CELL^{TM} cell viability analyser (Beckman Coulter, Krefeld, Germany).

3.5.3 Isolation and culture of Kupffer cells

Initially, rat livers were digested by rinsing with 80 mg of Collagenase in 100 ml rinsing buffer. Subsequently, liver was resected and stored in 100 ml ice cold PBS. After gentle mincing and filtration (150 μm mesh) hepatocytes were separated from non parenchymal cells by centrifugation for 5 min at 50 g and 40°C. Remaining supernatant was centrifuged for 10 min at 500 g and the pellet was resuspended in 40 ml medium (containing DMEM, 10% FBS, 1% glutamin and 1% Pen/Strep). The resulting suspension was transferred to a cell culture vessel to allow cells to adhere for 1 h at 37°C in an incubator. Afterwards endothelial cells were removed by adding 7 ml of trypsin solution. Remaining Kupffer cells were washed with medium, suspended by scraping and centrifuged for 10 min at 500 g. Finally, 15 ml of medium were added; cells were resuspended and cultivated in cell culture vessels. Cultivation was done according to cell culture with RAW 264.7 macrophage cell line.

3.6 Rat animal models

6 week old male Sprague-Dawley rats weighing 190 - 220 g were purchased from Charles-River-laboratories (Sulzfeld, Germany) and housed in a 12 h/ 12 h day/night cycle with free access to food (Ssniff, Soest, Germany) and tap water.

All animals received human care in compliance with the "Principles of Laboratory Animal Care". Studies were registered and approved by the government authorities.

3.6.1 Materials

Table 4   Materials used for animal studies

Product	Company
Fentanyl	Janssen-Cilag, Neuss, Germany
Midazolam	Ratiopharm, Ulm, Germany
Isofluran	Abbott, Wiesbaden, Germany
Carbogen (5% CO_2, 95% O_2)	Air Liquide, Duesseldorf, Germany

3.6.2 Biodistribution studies

Animals were anesthetized by i.p. injection of 0.005 mg/kg Fentanyl and 2.0 mg/kg Midazolam. For further maintainance of anesthesia, 1.5% Isofluran was continuously conducted using a vaporizer with Carbogen (5% CO_2/95% O_2) as a carrier gas. To obtain blood pressure and supervise anesthesia, the jugular artery was cannulated with a 16 gauge-PE catheter and connected to a blood-pressure gauge. The abdomen was opened by midline-laparotomy and the portal vein was prepared. 1.0 ml buffered gelatin-nanoparticle-solution containing 20 nmol Alexa Fluor® 488 5`-end-labeled NF-κB decoy oligonucleotides or unloaded Texas Red® labeled gelatin-nanoparticle-solution, respectively, was injected into the portal vein and organs and

blood samples were withdrawn after 15 minutes. Livers were drained, rinsed free from blood with PBS via a peristaltic pump at a flow of 55 ml/min for 2 minutes and perfused with Formalin 3% in PBS for protein fixation. Additionally, unfixed pieces of liver, kidney, brain, heart, spleen and lung tissues were withdrawn, cut in 3 mm cubes, immediately snap frozen in liquid nitrogen and kept at -80°C until further examination.

3.6.3 LPS

Anesthesia was performed as described in chapter 3.6.2. The abdomen was opened by midline-laparatomy and the portal vein was prepared. Throughout the experiment the body temperature was maintained between 36.0°C and 37.0°C with a warming lamp.

1.0 ml of a 20 nmol NF-κB decoy ODN nanoparticle-solution, a 20 nmol scrambled NF-κB decoy ODN nanoparticle-solution, unloaded "naked" nanoparticle-solution or solvent, respectively, were injected into the portal vein with a 1.0 ml syringe over a period of 5 minutes.

15 minutes thereafter 10 μg of LPS (50 μg/ml in PBS, E.coli serotype 055:B05) was applied to the portal vein. Following a 30 minutes incubation period, blood and liver tissue samples were collected and further treated as described in chapter 3.6.2.

After centrifugation of blood samples at 5000 U/min for 8 minutes, the plasma was stored in aliquots at -80°C.

3.6.4 Ischemia/reperfusion injury

Anesthesia was performed as described in chapter 3.6.2. The abdomen was opened by midline-laparotomy and the portal triad was prepared. Throughout the experiment the body temperature was maintained between 36.0°C and 37.0°C with a warming lamp.

The arterial and portal blood flow to the left lateral and median lobe of the liver was interrupted by applying an atraumatic clip, resulting in a 70% liver ischemia. After 60 minutes of ischemia, the blood supply was restored by removal of the clip and the reperfusion period was initiated.

Subsequently to the collection of blood samples into heparinized tubes, animals were sacrificed after 120 minutes of reperfusion by bleeding. The organ was rinsed free from blood by perfusing the liver with PBS through the portal vein via a peristaltic pump at a flow of 55 ml/min for 2 minutes. The median lobe was excised and the remaining lobes were perfused with formalin 3% in PBS for protein fixation.

All tissues were cut in 3 mm cubes, immediately snap frozen in liquid nitrogen and kept at -80°C until further examination.

After centrifugation of blood samples at 5000 U/min for 8 minutes, the plasma was stored in aliquots at -80°C.

15 minutes prior to initiation of ischemia, 1.0 ml of a 20 nmol decoy ODN nanoparticle-solution, a 20 nmol scrambled decoy ODN nanoparticle-solution, unloaded "naked" nanoparticle-solution and solvent, respectively, were injected into the portal vein with a 1.0 ml syringe over a period of 5 minutes (Figure 6).
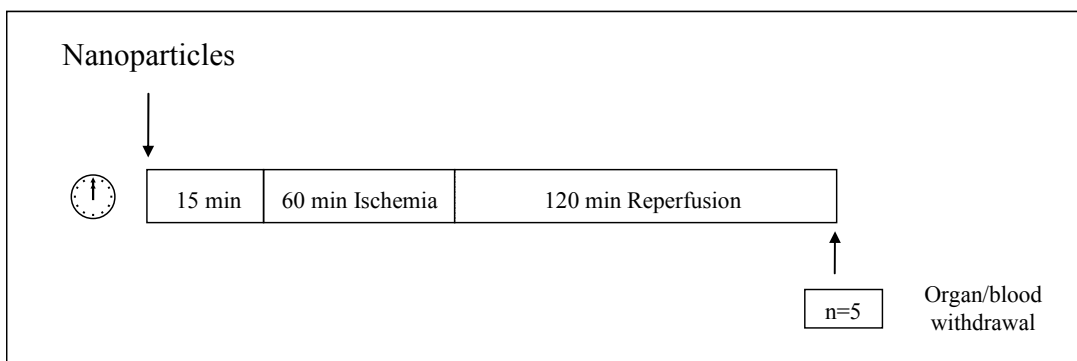
Figure 6   Experimental setting of ischemia/reperfusion

3.7 Immunohistochemistry

3.7.1 Materials

Table 5   Materials used for immunohistochemistry

Product	Company
Hoechst 33342	Invitrogen, Karlsruhe, Germany
Permafluor® mounting medium	Beckman Coulter, Krefeld, Germany
Triton® X-100	Sigma-Aldrich, Taufkirchen, Germany

3.7.2 Antibodies

Table 6   Primary antibodies used for immunohistochemistry

Product	Company
p65 (RB-9034) rabbit polyclonal IgG	Labvision, Fremont, USA
CD 163 (MCA342R) mouse anti-rat IgG	AbD Serotec GmbH, Duesseldorf, Germany

Table 7   Secondary antibodies used for immunohistochemistry

Product	Company
Alexa Fluor® 488 goat anti-mouse IgG	Invitrogen, Karlsruhe, Germany
Alexa Fluor® 546 goat anti-rabbit IgG	Invitrogen, Karlsruhe, Germany
Alexa Fluor® 633 goat anti-mouse IgG	Invitrogen, Karlsruhe, Germany

3.7.3 Staining of isolated Kupffer cells

At first, cover slips were placed in each well of 24-well plates. Subsequently, Kupffer cells acquired from isolation process ($\sim 0.3 \times 10^6$ cells/ml) were equally distributed to prepared well plates. Each well was completed with medium (DMEM

containing 10% of FBS and 1% of glutamin) to a total volume of 500 µl. After 1 h of adherence to the cover slips, cells were washed with medium once and 450 µl medium were added. Cells were then incubated with 50 µl of an NF-κB decoy ODN$_{488}$ loaded fluorescent gelatin nanoparticle suspension. The final decoy ODN concentration per well was adjusted to 0.5 µmol/l, i.e. 3.7 µg ODN per well. The according nanoparticle concentration resulting from 2.5% [m/m] drug loading accounted for 148.4 µg gelatin nanoparticles per well. After 15 min, 1 h and 2 h respectively of incubation, cells were fixed with 3% formalin in PBS for 10 min and washed thrice with PBS.

Subsequent to fixing and washing, Kupffer cells were permeabilized for 2 min with 0.2% Triton® X in PBS and washed three times with PBS. Nuclear staining was then performed by incubating cells with 10 µl Hoechst solution (50 µg/ml) in 500 µl PBS for 10 min. Following final washing for three times with PBS, cover slips were taken from well plates and were fixed with PermaFluor® mounting medium on a microscopic slide. After storing over night, the Kupffer cell preparations were analyzed with a Zeiss LSM 510 Meta confocal laser scanning microscope (Carl Zeiss Microscope Systems, Jena, Germany).

3.7.4 Staining of liver tissue

3.7.4.1 p65

Formalin-fixed, paraffin embedded liver samples were cut into 8 µm thick slices. After deparaffinization in xylene and rehydration through a declining ethanol-series, slices were stained using Coverplate^{TM} disposable immunostaining chambers (Thermo Shandon, Frankfurt, Germany). For evaluation of NF-κB-activation, sections were first incubated with a 1:50 dilution of a rabbit polyclonal p65-antibody and a 1:100 dilution of a mouse anti-rat monoclonal CD 163-antibody in 0.2% saline buffered BSA overnight at 4°C. After repeated washing with PBS, the secondary antibodies Alexa® 488 goat anti-mouse and Alexa® 546 goat anti-rabbit in 0.2% saline buffered BSA were applied for 45 minutes, followed by staining of nuclei with

Hoechst for further 5 minutes. All sections were mounted with PermaFluor® Mounting Medium and analyzed by confocal laser scanning microscopy (Zeiss LSM 510 Meta CLSM, Carl Zeiss Microscope Systems, Jena, Germany).

3.7.4.2 Distribution of labeled nanoparticles

For evaluation of decoy nanoparticle biodistribution, slices were treated accordingly as in section 3.7.4.1 (primary antibody mouse anti-rat monoclonal CD 163 diluted 1:100, AbD Serotec, and secondary antibody Alexa® 488 goat anti-mouse diluted 1:400, Invitrogen).

3.7.4.3 Distribution of labeled decoy nanoparticles

For evaluation of decoy nanoparticle biodistribution, slices were treated accordingly as in section 3.7.4.1 (primary antibody mouse anti-rat monoclonal CD 163 diluted 1:100, AbD Serotec, and secondary antibody Alexa® 633 goat anti-mouse diluted 1:400, Invitrogen).

3.8 EMSA

3.8.1 Materials and solutions

Table 8   Materials used for electro mobility shift assay

Product	Company
[γ32P]-ATP 3000 Ci/mmol	Amersham, Freiburg, Germany
Nuc Trap probe purification columns	Stratagene, La Jolla, USA
T4 polynucleotide kinase	USB, Cleveland, USA
Oligonucleotides	Promega, Heidelberg, Germany

Buffer A

10 mM	Hepes	pH 7.9
10 mM	KCl	
0.1 mM	EDTA	
0.1 mM	EGTA	
	H_2O	

add freshly before use:

1 mM	DTT
0.5 mM	PMSF

Buffer B

20 mM	Hepes	pH 7.9
400 mM	NaCl	
1 mM	EDTA	
0.5 mM	EGTA	
25 %	Glycerol	

add freshly before use:

1 mM	DTT
1 mM	PMSF

STE buffer   pH 7.5

10 mM	Tris
100 mM	NaCl
1 mM	EDTA
	H_2O

Binding Buffer 5x

20 %	Glycerol
5 mM	$MgCl_2$
2.5 mM	EDTA
250 mM	NaCl
50 mM	Tris-HCl
	H_2O

Reaction buffer

90 %	Binding buffer 5x
10 %	Gel loading buffer
2.6 mM	DTT
	H_2O

Gel loading buffer

250 mM	Tris-HCl
0.2 %	Bromphenolblue
40 %	Glycerol
	H_2O

Non-denaturizing	PAA gel		TBE 10x	
5.3 %	TBE 10x		890 mM	Tris
15.8 %	PAA solution 30%		890 mM	Boric acid
2.6 %	Glycerol		20 mM	EDTA
0.05 %	TEMED			H_2O
0.08 %	APS			
	H_2O			

3.8.2 Extraction of nuclear protein from RAW 264.7 macrophages

RAW 264.7 macrophages were grown in 6-well plates until confluence, and incubated with 1 nmol decoy nanoparticles and scrambled decoy nanoparticles, respectively, for 3 hours. Then 2 µg LPS (100 µg/ml) were added to each well, leading to a final concentration of 100 ng/ml. Subsequent to a 30 minute waiting period, plates were put on ice and cells were washed twice with ice-cold PBS, scraped off in PBS with a rubber cell scraper, centrifuged for 5 minutes at 1,500 rpm at 4°C and resuspended in 400 µl Buffer A for 15 minutes. Then 25 µl Nonidet P-40 was added, intensively vortexed and centrifuged (12,000 rpm, 1 minute, 4°C). The supernatant was discarded and the nuclear pellet was resuspended in 50 µl Buffer B and vortexed. After 30 minutes of continuous shaking at 4°C, the nuclear extract was centrifuged for 5 minutes at 12,000 rpm. The supernatant containing the nuclear proteins was stored in aliquots at -80°C.

3.8.3 Extraction of nuclear protein from liver tissues

Tissue samples (approx. 60-80 mg) were prepared with a homogenizer (Potter S, B. Braun Biotech) by homogenizing the probes in 600-800 µl Buffer A. After

centrifugation (1,000 rpm, 10 minutes, 4°C) and incubation at 4°C for 10 minutes in 300 µl freshly added Buffer A containing 18 µl of NP-40 10 %, probes were centrifuged (14,000 rpm, 10 minutes, 4°C). The supernatant was removed and the pellet was suspended in Buffer B, following incubation at 4°C for 30 minutes under continuous shaking. After centrifugation (14,000 rpm, 10 minutes, 4°C) supernatants were frozen at -80°C and nuclear proteins were stored until further use for protein quantification and EMSA.

3.8.4 Protein quantification

Protein concentrations in isolated nuclear protein fractions were determined by the method of Bradford using Coomassie brilliant blue G250. Absorbance of the samples was measured at 590 nm (Tecan Sunrise Absorbance reader, Tecan).

3.8.5 Radioactive labeling of consensus oligonucleotides

Double-stranded oligonucleotides containing the consensus sequence for NF-κB 5'- AGT TGA GGG GAC TTT CCC AGG C -3' were 5' end-labeled with [γ^{32}P]-ATP using the T4 polynucleotide kinase which catalyzes the transfer of the radioactive phosphate to the 5' hydroxyl site of the DNA. After incubation of oligonucleotides with T4 kinase for 10 minutes at 37°C, the reaction was terminated by addition of 0.5 M EDTA solution. The radioactive labeled DNA was separated from unlabeled DNA by using Nuc Trap probe purification columns. Radioactive oligonucleotides were eluted from the column with 70 µl of STE buffer and frozen at -20°C until used for EMSA.

3.8.6 Binding reaction and electrophoretic separation

To ensure equal amounts of proteins, 30 µg (liver tissue) and 5 µg of protein (RAW 264.7 macrophages), respectively, were provided in a total amount of 14 µl,

containing 2 µg poly(dIdC) and 3 µl of freshly prepared reaction buffer. Then, samples were incubated for 10 minutes at room temperature. To start NF-κB – DNA binding reaction, 1 µl of the radioactive labeled oligonucleotide was added and samples were left for 30 minutes at room temperature. The protein-oligonucleotide complexes were separated by gel electrophoresis (Mini-Protean 3, BioRad) with 0.25 x TBE buffer at 100 V for 60 minutes using non-denaturizing polyacrylamide gels.

For supershift analysis, 1 µl of an antibody against p50 or p65, respectively, was incubated with the nuclear protein for 30 minutes, before adding the radioactive labeled probe. Electrophoretic separation was done as described above.

3.8.7 Detection and evaluation

Following electrophoresis, gels were exposed to Cyclone Storage Phosphor Screens (Canberra-Packard, Schwadorf, Austria) for 24 hours, followed by analysis with a phosphor imager station (Cyclone Storage Phosphor System, Canberra-Packard).

3.9 Real time RT-PCR

3.9.1 Primers

TNF-α primers and probe were obtained as a complete TaqMan® Gene Expression Assay (Rn99999017_m1, Applied Biosystems, Hamburg, Germany). GAPDH primers were designed using the Primer Express® 2.0 software program. GAPDH forward primer: 5'-GGG AAG GTG AAG GTC GGA GT-3'; reverse primer: 5'-TCC ACT TTA CCA GAG TTA AAA GCA G-3'; probe: 5'-ACC AGG CGC CCA ATA CGA CCA A-3'.

3.9.2 RNA isolation and sample preparation

25 mg of liver tissue were used to isolate mRNA by using the RNeasy® Mini Kit (Qiagen, Hilden, Germany) according to the manufacturers` instructions. Homogenized tissue samples were loaded onto a QIAshredder Spin Column and spun down (14,000 rpm, 2 minutes, RT) to ensure complete homogenization. The extracts were then applied to the RNeasy® mini columns. Following several washing and centrifugation steps, the RNA bound to the RNEasy® Mini Spin Columns was eluated with RNAse free water. DNAse digestion was performed during isolation with RNAse-free DNAse set from Qiagen. Content of isolated RNA was determined by UV-spectroscopy at 260 nm/ 280 nm with a NanoDrop® ND-1000 Spectrophotometer, NanoDrop Technologies, Wilmington, USA (kindly provided by the GSF – National research center for environment and health, Großhadern).

3.9.3 Reverse transcription

Reverse transcription was carried out using the High Capacity cDNA Reverse Transcription Kit (Applied Biosystems, Hamburg, Germany) in a 7300 Real-Time PCR System (Applied Biosystems, Hamburg, Germany). Total amount of RNA deployed was 1,500 ng in 30 µl of reaction buffer containing 2x RT buffer, $MgCl_2$, dNTP Mix, random hexamers, RNAse inhibitor and reverse transcriptase enzyme.

Table 9   Cycling protocol for reverse transcription into cDNA

Purpose	Temperature	Time
Primer extension	25°C	10 minutes
cDNA synthesis	48°C	30 minutes
Reaction termination	95°C	5 minutes

3.9.4 Real-time PCR

Real time PCR was conducted with the TaqMan® Universial Master Mix Kit in a 7300 Real-Time PCR System (Applied Biosystems, Hamburg, Germany). In total 100 ng of cDNA in 20 µl of reaction buffer containing 2 x Master Mix and the according forward and reverse primers as well as the corresponding TaqMan Probe was deployed.

Table 10   Cycling protocol for real time RT-PCR analysis

Purpose	Temperature	Time	
Initial denaturizing	95°C	10 minutes	
Denaturizing	95°C	15 seconds	50 cycles
Annealing and extension	60°C	60 seconds	

3.9.5 Quantification

Results were quantified based on the relative expression of the TNF-α gene versus the housekeeping gene GAPDH using the mathematical model for relative quantification according to Pfaffl (104).

3.10 ELISA

Rat TNF-α UltraSensitive ELISA Kit was obtained from BioSoure, Camarillo, USA. Determination of serum TNF-α levels was performed according to the manufacturers manual. Briefly, after centrifugation of heparinized blood samples for 8 minutes at 5,000 rpm, the supernatant was separated and stored at -80°C until further analysis. Then 50 µl incubation buffer and 50 µl biotin conjugate were added to each 50 µl serum sample. Following a waiting period for 2 hours and several washing steps, the samples were incubated with 100 µl streptavidin coupled horse radish peroxidase for

30 minutes. After further washing steps, 100 µl of stabilized chromogen were added to each well, causing a color development proportional to the amount of rat TNF-α in the sample. Finally, reaction was terminated by adding 100 µl of stop solution and the absorbance was measured at 450 nm using the SUNRISE Absorbance Reader from TECAN (TECAN Deutschland GmbH, Crailsheim, Germany).

3.11 Measurement of transaminases

Activities of serum aminotransferases (alanine transferase (ALT) and aspartate transferase (AST)) were determined as established markers of hepatic injury. Activities of heparinized serum were kindly measured by Babett Rannefeld from the Institute for clinical chemistry, Klinikum Großhadern, University of Munich, Germany, using a serum multiple analyzer (Olympus AU 2700, Germany) at 37 °C.

3.12 Gene Chip analysis

Isolation of RNA, reverse transcription and the following Gene Chip analysis is kindly conducted by Dr. H. Blum, Dr. S. Bauersachs and A. Klanner from the Laboratory for Functional Genome Analysis (Lafuga).

3.12.1 Isolation of RNA

RNA was extracted using the RNeasy Kit (Quiagen, Hilden, Germany) and Trizol (Invitrogen, Karlsruhe, Germany). Liver samples weighing about 200 – 300 mg from each animal were added to 1 ml of pre-chilled Trizol Reagent. Total RNA extractions were performed according to the manufacturer's protocol and were further purified by passage through RNeasy mini-columns. Final RNA preparations were resuspended in RNase-free water and stored at -80°C. The concentration of extracted

RNA was quantified spectrophotometrically, and purity and integrity was assessed by agarose gel electrophoresis. All samples showed 260/280 absorbance ratios of approximately 2.0, and all displayed intact ribosomal 28S and 18S RNA bands in an ratio of about 2:1 as seen by ethidium bromide staining.

3.12.2 Reverse transcription and hybridization

Double-stranded cDNA was synthezised using the Affymetrix kit (Affymetrix, Santa Clara, USA), starting with samples of 10 µg of total RNA. An in vitro transcription (IVT) reaction was carried out to produce biotin-labelled cRNA from the cDNA according to the manufacturer's protocol (http://www.affymetrix.com/support/technical/manual/expression_manual.affx). After fragmentation of cRNA, 10 µg of biotin-labelled cRNA probe are hybridized with an Affymetrix GeneChip according to the companys standard procedure. After washing, the hybridized probe arrays are counterstained with streptavidin phycoerythrin conjugate and scanned with a Typhoon scanner (GE Healthcare, Munich, Germany).

3.13 Statistical analysis

Number of experiments is depicted in the respective figure legend. Results are shown as mean ± SEM. Statistical analysis was performed using the GraphPad Prism 3.03 software (GraphPad software Inc, San Diego, USA). Significance (*) has always been calculated at the 95% confidence interval between indicated groups, using an unpaired t-test.

4 RESULTS

4.1 In vitro uptake: isolated Kupffer cells

We first aimed to check if gelatin nanoparticles are taken up in general by Kupffer cells. Therefore, Kupffer cells were isolated from rat liver to investigate phagocytosis of nanoparticles in vitro. To this end, gelatin nanoparticles were incorporated with a Texas Red X fluorescent dye and additionally loaded with Alexa® 488 fluorescent labeled decoys. Analysis by confocal microscopy revealed a pronounced uptake after 15 minutes incubation time already (Figure 7). In addition, some decoys seem to be detached from the gelatin nanoparticles and to translocate to the nucleus, as several fluorescent decoy oligonucleotides could be found in the nuclear compartment separated from the carrier. The uptake as well as the translocation of decoys to the nucleus was further enhanced in a time-dependent kinetic pattern.
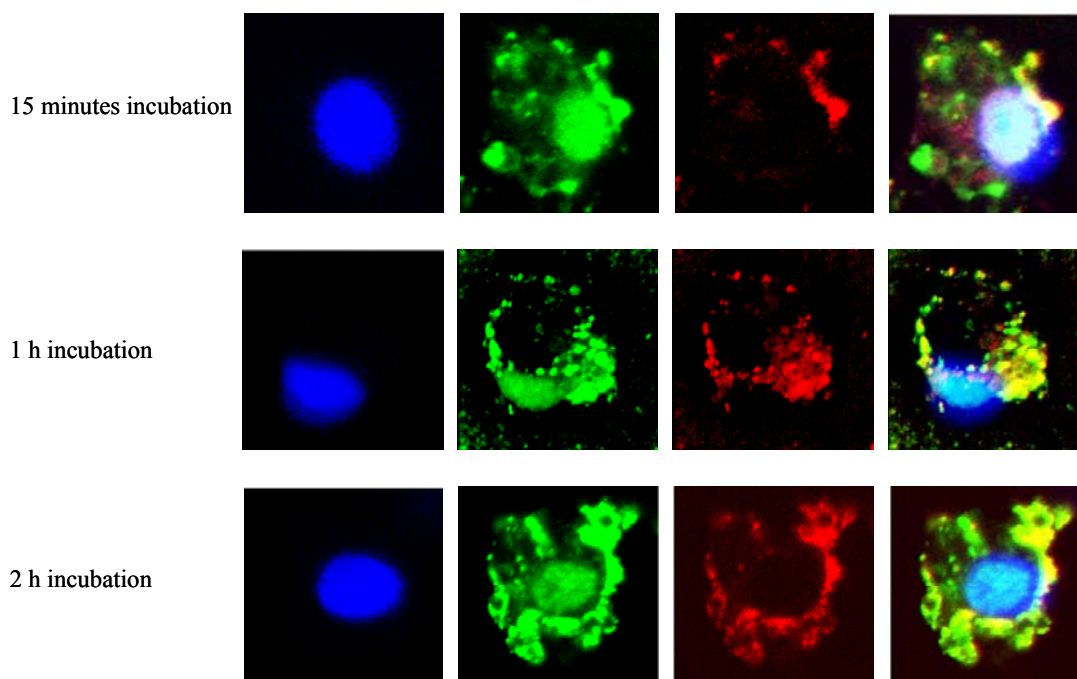

Figure 7   Time-dependent uptake of NF-κB decoy nanoparticles in isolated Kupffer cells. Stimulation and staining of Kupffer cells was performed as described in chapter 3.7.3. Blue: nuclei, green: decoy ODNs, red: gelatin nanoparticles. The yellow colour indicates colocalization of decoy ODNs and nanoparticles.

4.2 In vivo distribution

4.2.1 Gelatin nanoparticles

Since a distinct uptake of gelatin nanoparticles by Kupffer cells in vitro is to be seen as soon as 15 minutes after the challenge, we wanted to figure out if an analogue uptake pattern can be observed in vivo. Therefore, a Texas Red X fluorescent dye was incorporated into the gelatin nanoparticles and 1.0 ml of a buffered saline nanoparticle-solution was injected into the portal vein. Examination of confocal microscope images showed a clear uptake of gelatin nanoparticles by Kupffer cells, whereas the surrounding parenchyma remains completely unaffected (Figure 8).

Nanoparticles   Kupffer cells   Overlay
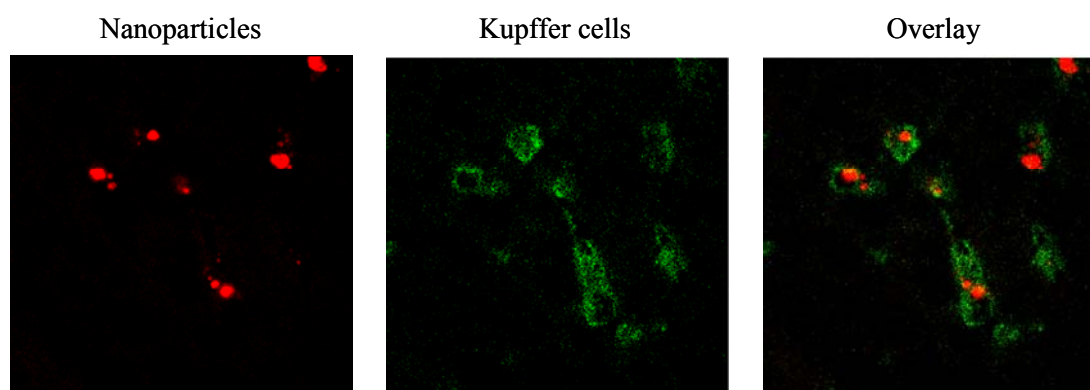
Figure 8   Gelatin nanoparticles are selectively taken up in the liver by Kupffer cells. Staining and confocal microscopy was performed as described in chapter 3.7.4. Red: gelatin nanoparticles, green: Kupffer cells.

4.2.2 Decoy nanoparticles

Since we showed a distinct hepatic uptake of gelatin nanoparticles by Kupffer cells, we aimed to test if the loaded decoy oligonucleotides are still bound stably to the nanoparticles under in vivo conditions. Therefore, an Alexa® 488 fluorescent dye was attached to the decoy oligonucleotides and the distribution of decoy loaded nanoparticles was evaluated.

4.2.2.1 Systemic distribution

In our approach, decoy nanoparticles are injected intraportally, thus entering the systemic circulation. Although the liver is the first organ to be reached by administration into the portal vein, a delivery to other organs can not be ruled out. Therefore we wanted to investigate the whole body distribution of systemically applied decoy nanoparticles 15 minutes after injection. Fluorescent labeled decoy oligonucleotides loaded onto gelatin nanoparticles were localized to a predominant extent in hepatic tissue (Figure 9). Some decoy oligonucleotides were detected in the lung and the spleen, but kidney, heart and brain tissues were not affected at all.

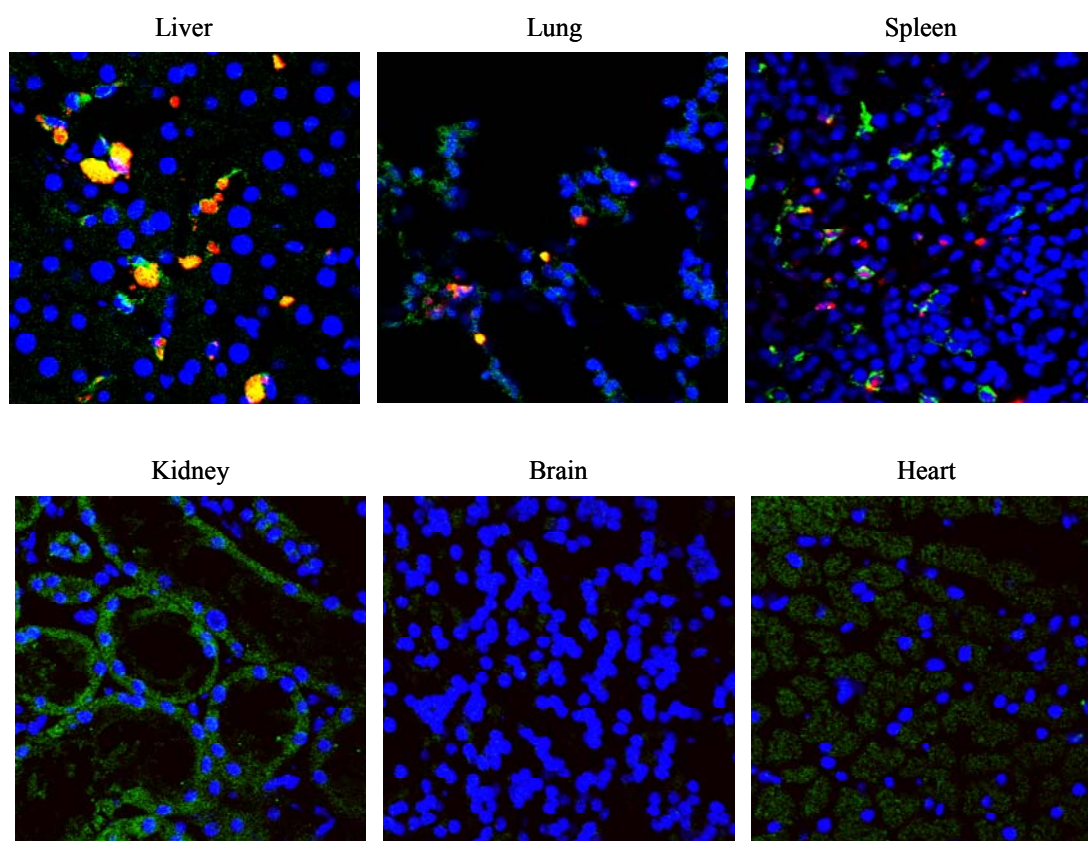Figure 9   Intraportal administration of decoy nanoparticles results in enhanced distribution in liver tissue. Staining and confocal microscopy was performed as described in chapter 3.7.4. Red: decoy ODNs, green: Kupffer cells and macrophages, blue: nuclei. The yellow colour indicates colocalization of decoy ODNs and macrophages.

4.2.2.2 Intrahepatic localization

As the liver is the main organ affected by intraportal injection, we wanted to clarify in the next step if Kupffer cells are the predominant liver cell type targeted. And indeed, as displayed in Figure 10, a colocalization of decoys and Kupffer cells in vivo 15 minutes after application of gelatin nanoparticles loaded with decoy oligonucleotides is clearly to be seen, as indicated by the yellow colour. There were no decoys found in hepatocytes or endothelial cells.

| Decoys | Kupffer Cells | Nuclei | Overlay |
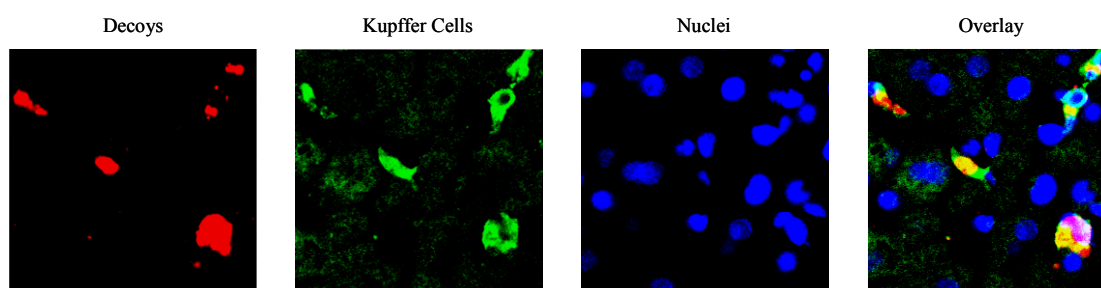
Figure 10 Decoy nanoparticles are selectively taken up in the liver by Kupffer cells. Staining and confocal microscopy was performed as described in chapter 3.7.4. Red: decoy ODNs, green: Kupffer cells, blue: nuclei. The yellow colour indicates colocalization of decoy ODNs and Kupffer cells.

4.2.3 DOTAP/DOPC liposomes

DOTAP/DOPC liposomes are widely used carriers for oligonucleotides. Hence, we wanted to compare the efficiency of the state-of-the-art liposomal delivery to our gelatin nanoparticulate carrier. Fluorescent labeled decoy oligonucleotides were incorporated into DOTAP/DOPC liposomes and administered intraportally. Analysis by confocal imaging (Figure 11) showed an increased loss of decoy oligonucleotides within the sinusoid as well as an enhanced uptake by hepatocytes and endothelial cells (yellow arrows) in comparison to the use of gelatin nanoparticles as ODN-carrier.

Thus, gelatin nanoparticles indeed are the superior carrier for a selective targeting of Kupffer cells.

Decoys	Kupffer Cells	Nuclei	Overlay

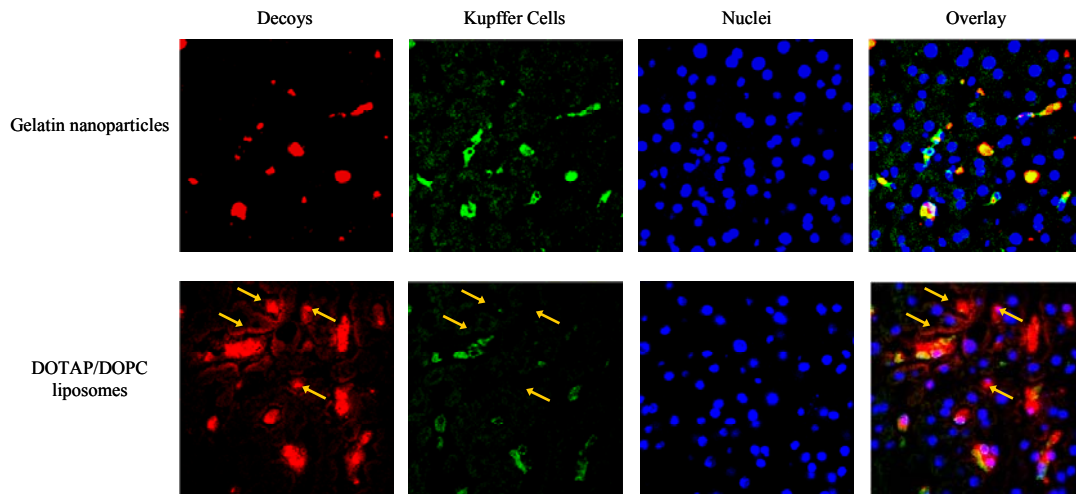Figure 11 Use of DOTAP/DOPC liposomes as carrier for incorporated decoy ODNs results in increased loss of decoys as well as in enhanced delivery to many liver cell types (yellow arrows). Staining and confocal microscopy was performed as described in chapter 3.7.4. Red: decoy ODNs, green: Kupffer cells, blue: nuclei. The yellow colour indicates colocalization of decoy ODNs and Kupffer cells.

4.3 In vitro: Decoy nanoparticles and LPS – RAW macrophages

As we were able to confirm that decoy oligonucleotides are delivered to the liver macrophages by gelatin nanoparticles, we now aimed to test whether decoy nanoparticles are also able to inhibit NF-κB in vitro. To this end, a RAW 264.7 cell line was used as a model for a macrophage cell type and stimulated with LPS, a well known inducer of NF-κB binding activity.

4.3.1 Composition of the NF-κB dimer in LPS challenged RAW macrophages

The transcription factor NF-κB is composed of two subunits and forms either hetero- or homodimers. To determine the composition of the dimer after LPS challenge in this cell line, the nuclear proteins from RAW 264.7 macrophages stimulated with LPS were extracted. EMSA supershift analysis (Figure 12) revealed that the investigated NF-κB complex consists of the subunits p50 and p65, as the respective

antibody effectuates a strong decline in the radioactive signal intensity (middle and right lane) in comparison to the not-shifted band (left lane).
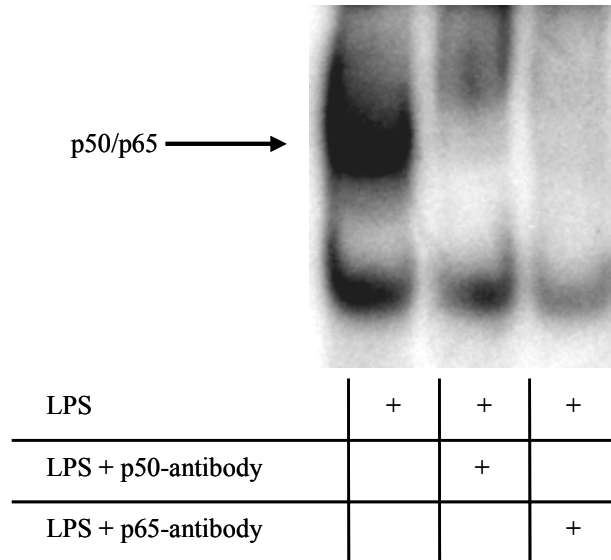

	LPS		
LPS	+	+	+
LPS + p50-antibody		+	
LPS + p65-antibody			+

Figure 12 The transcription factor NF-κB is composed of the two subunits p50 and p65. Stimulation of RAW 264.7 macrophages, protein extraction and determination of NF-κB binding activity by electromobility shift assay (EMSA) was performed as described in section 3.8.

4.3.2 NF-κB decoy oligonucleotides bind NF-κB

The NF-κB decoy oligonucleotide sequence we wanted to apply possesses two NF-κB binding sites, one for p50 and the other for p65. As shown in Figure 12, the LPS induced NF-κB complex consists of these two subunits. To verify that the used NF-κB decoy oligonucleotides are able to bind to the activated NF-κB proteins, nuclear extracts of RAW 264.7 macrophages stimulated with LPS were incubated with 1.75 pmol of decoy oligonucleotides for 15 minutes. The radioactive labeled NF-κB binding oligonucleotides added thereafter were not able to bind to NF-κB. This suggests that the decoy oligonucleotides applied in an equimolar amount replace the radioactive labeled probe, therefore proofing the selective binding of the decoy oligonucleotide sequence. Scrambled decoy oligonucleotides were not able to hinder the radioactive labeled probe from binding the NF-κB protein as much as the binding decoy oligonucleotides, indicating the sequence specifity. However, a small decrease

in signal intensity can be observed by the use of scrambled decoy oligonucleotides. This can be explained by the large amount of oligonucleotides used in this experiment, which inevitably leads to an unselective interaction.

LPS	+	+	+
scrambled Decoy Oligonucleotide		+	
Decoy Oligonucleotide			+
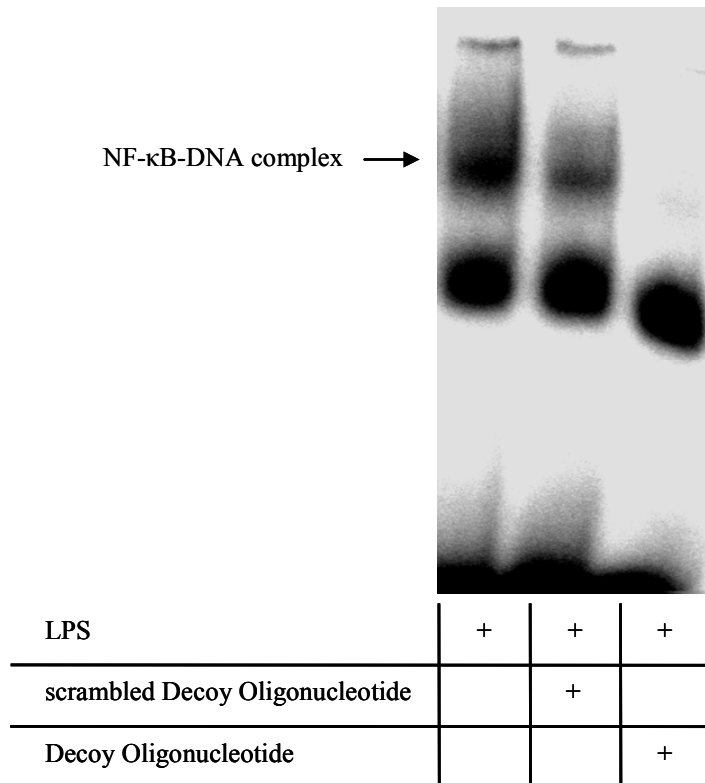
Figure 13 Addition of 1 µl of double stranded NF-κB decoy oligodeoxynucleotide hinders radioactive labeled NF-κB consensus oligonucleotides from binding to NF-κB. Stimulation of RAW 264.7 macrophages, protein extraction and determination of NF-κB binding activity by electromobility shift assay (EMSA) was performed as described in section 3.8.

4.3.3 Decoy nanoparticles reduce LPS induced NF-κB activity in vitro

We determined the influence of decoy nanoparticles on NF-κB binding activity in vitro upon LPS stimulation by EMSA. Figure 14 displays that the elevation of NF-κB activity could be strongly diminished by the application of decoy nanoparticles before the LPS challenge. Scrambled decoy nanoparticles showed only a slight impact on NF-κB activity in vitro, which demonstrates that the degree of NF-κB inhibition is sequence dependent. As described in the section above, the presence of random oligonucleotides to such an extent seems to be sufficient to

influence NF-κB binding activity moderately. However, the use of NF-κB decoy oligonucleotides results in a much more prominent downregulation of NF-κB.

	LPS	+	+	+		
Decoy-NP			+		+	
scrambled Decoy-NP				+		+
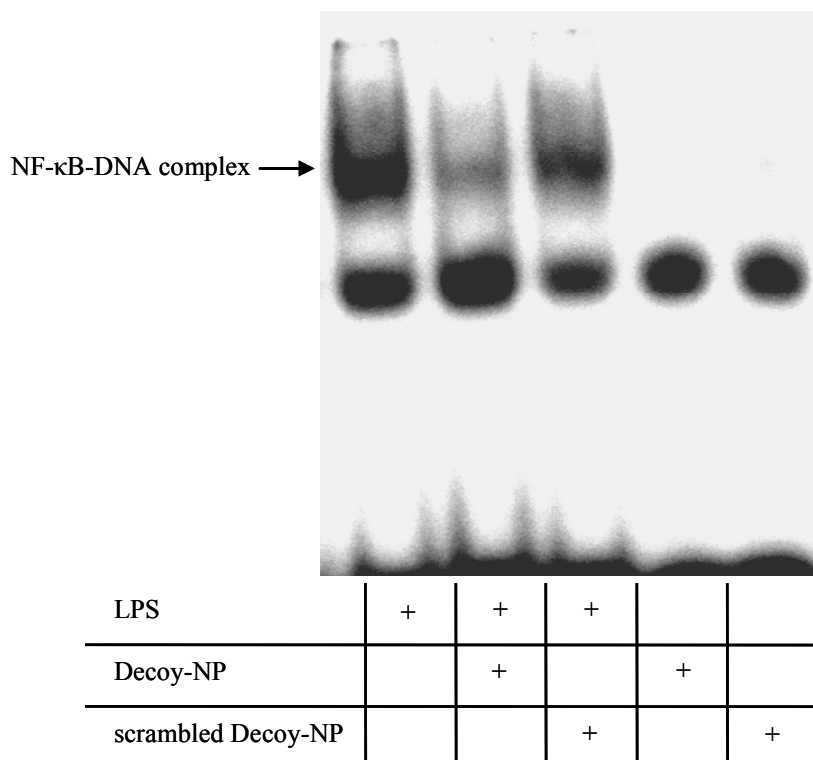
Figure 14 Addition of 1 μM decoy nanoparticles 3 h before LPS challenge reduces NF-κB binding activity. Stimulation of RAW 264.7 macrophages, protein extraction and determination of NF-κB binding activity by electromobility shift assay (EMSA) was performed as described in section 3.8.

4.4 In vivo: Decoy nanoparticles and LPS

After establishing that (i) the gelatin nanoparticles are an appropriate Kupffer cell targeting carrier for decoy oligonucleotides in vitro and in vivo and that (ii) application of decoy nanoparticles inhibits NF-κB binding activity in vitro, we next aimed to investigate if decoy nanoparticles display an inhibitory action in vivo as well. As LPS is a well-known and reliable stimulus of NF-κB activation in Kupffer cells, we utilized an LPS-model to supply the proof of principle for a Kupffer cell specific NF-κB inhibition by decoy nanoparticles.

4.4.1 Induction of NF-κB activity by LPS

We determined the increase in NF-κB binding activity by EMSA after the challenge with different doses of LPS (Figure 15). As we aimed to simulate a mild inflammatory reaction, we decided to use a dose of 10 μg LPS for further experiments. This low quantity is sufficient to induce NF-κB activity without causing a severe sepsis.

NF-κB-DNA complex ⟶

LPS (μg)   200   50   10   --
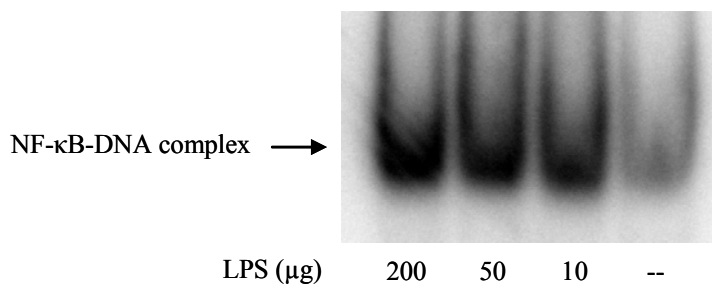
Figure 15 Systemic application of LPS induces hepatic NF-κB binding activity. Protein extraction and determination of NF-κB binding activity by electromobility shift assay (EMSA) was performed as described in chapter 3.8.

4.4.2 Influence on NF-κB activity

Intraportal administration of LPS lead to a clear increase in NF-κB binding activity (Figure 16). However, this induction can be completely abolished by the prior application of decoy nanoparticles. Scrambled decoy and naked nanoparticles, respectively, showed no impact on NF-κB binding activity. To ensure comparability between the treated groups, decoy versus scrambled decoy nanoparticles were compared for future experiments, as differences in obtained results have to be due to the sequence specifity of the decoy oligonucleotide.
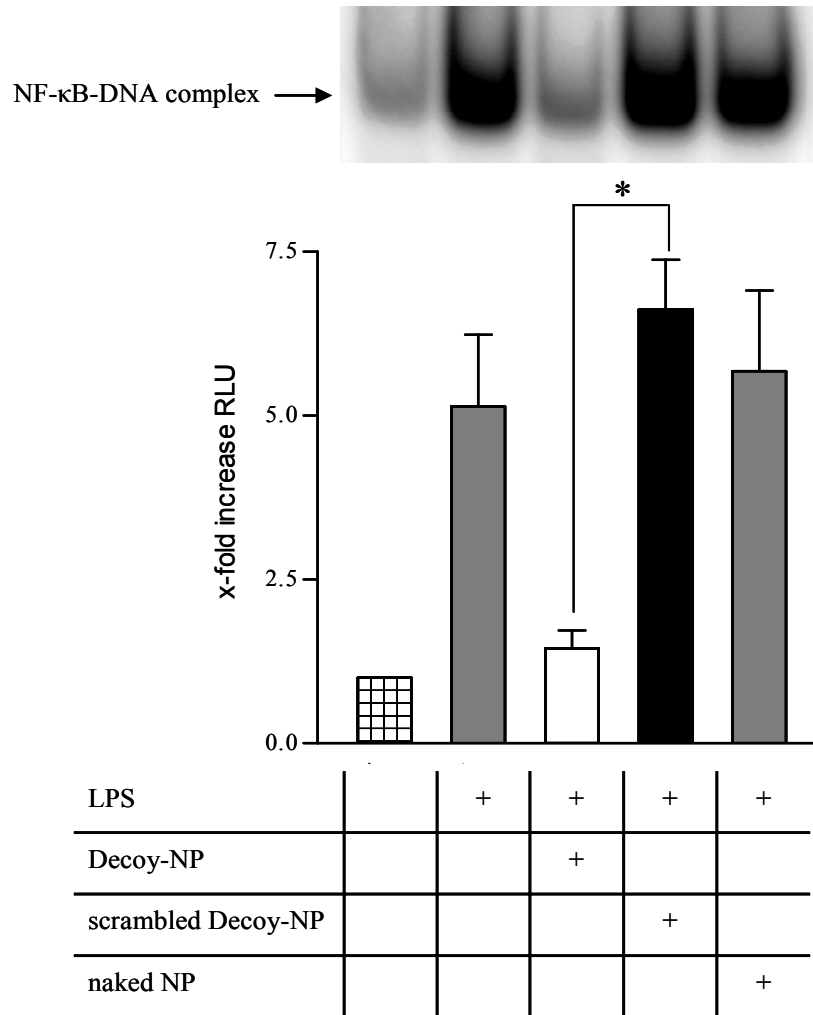
Figure 16 Administration of NF-κB decoy nanoparticles abolishes LPS induced NF-κB binding activity. Protein extraction and determination of NF-κB binding activity by electromobility shift assay (EMSA) was performed as described in section 3.8. All experiments were conducted three times. One representative EMSA blot is depicted above.

4.4.3 Decoy nanoparticles retain p65 within the cytoplasm

We next wanted to clarify the underlying mechanism of the NF-κB inhibition by decoy nanoparticles. Liver tissues treated with either scrambled decoy nanoparticles or decoy nanoparticles before the challenge with LPS were stained with an antibody against p65. Confocal microscopy showed that p65 seems to be detained from translocation to the nucleus (Figure 17). As the transcription factor NF-κB has to enter the nucleus in order to bind to its designated promoter region, a retention in the cytoplasm makes transcription impossible.

| | Nuclei | Kupffer cells | p65 | Overlay |
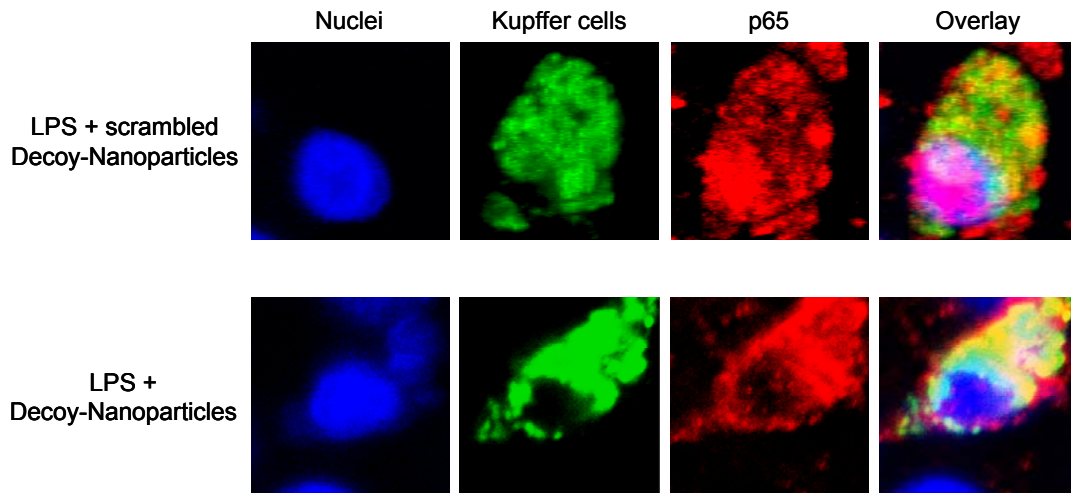
Figure 17 Decoy nanoparticles prevent p65 from entering the nucleus in Kupffer cells. Staining and confocal microscopy was performed as described in chapter 3.7.4. Blue: nuclei, green: Kupffer cells, red: p65. The purple colour indicates colocalization of p65 and nucleis.

4.4.4 Influence on TNF-α

4.4.4.1 TNF-α mRNA expression

The TNF-α gene is mainly regulated by the transcription factor NF-κB. Thus, a reduction in NF-κB activity should also lead to diminished TNF-α mRNA expression. To test this hypothesis we conducted a real-time RT PCR to measure TNF-α mRNA expression of hepatic tissue. Application of decoy nanoparticles indeed reduced the LPS provoked rise in TNF-α mRNA in comparison to the scrambled decoy nanoparticle group (Figure 18). Therefore, delivery of decoy oligonucleotides by gelatin nanoparticles selectively into Kupffer cells results in interaction with NF-κB mediated downstream pathways. Hence, we provided the proof of principle, as targeting of Kupffer cells with decoy nanoparticles indeed interferes with inflammatory signalling.
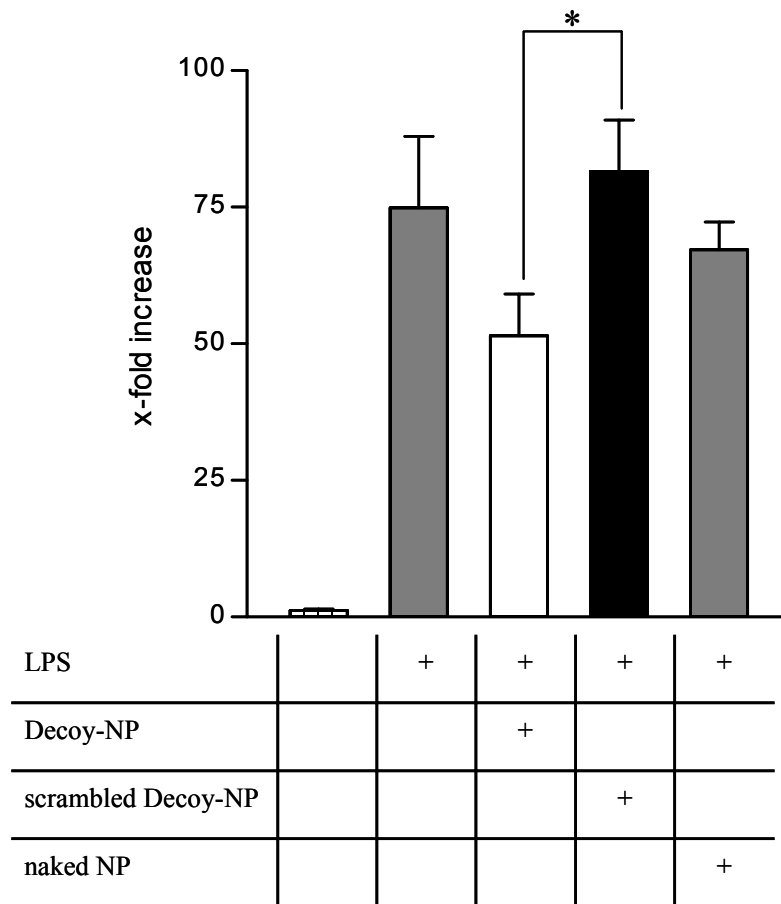
Figure 18 Administration of decoy nanoparticles diminishes LPS induced TNF-α mRNA expression. RNA isolation and real time RT-PCR were performed as described in chapter 3.9. Experiments were conducted five times.

4.4.4.2 TNF-α release

After the significant reduction of hepatic TNF-α mRNA expression by the intervention with decoy nanoparticles, analysis of TNF-α levels in the blood plasma by ELISA should provide information about the systemic TNF-α release. However, Figure 19 reveals that the systemic TNF-α levels were only tendencially reduced by decoy nanoparticles without reaching statistical significance.

The chart shows TNF-α pg/ml on the y-axis with the following experimental conditions:

		LPS	Decoy-NP	scrambled Decoy-NP	naked NP
LPS		+	+	+	+
Decoy-NP			+		
scrambled Decoy-NP				+	
naked NP					+
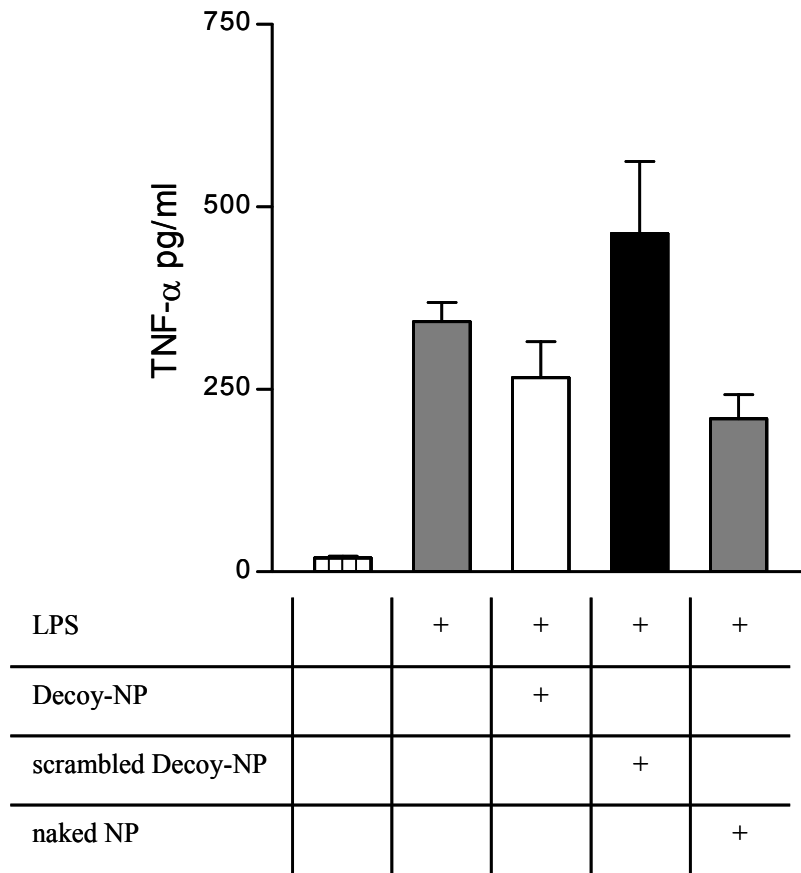
Figure 19 Systemic TNF-α release is not affected by decoy nanoparticles. ELISA of heparinized blood plasma samples was performed as described in chapter 3.10. Experiments were conducted three times.

4.5 In vivo: Decoy nanoparticles and hepatic ischemia/reperfusion

As we are able to interfere with inflammatory NF-κB mediated signalling pathways in Kupffer cells, we now used our tool to elucidate the impact of a selective NF-κB inhibition in the model of hepatic ischemia/reperfusion injury.

4.5.1 Establishment of a rat model of partial warm ischemia/reperfusion

Before we were able to investigate the impact of the decoy nanoparticles in another inflammatory liver setting, we had to set up a working model of warm ischemia/reperfusion and characterize its features. A stable anesthesia without affecting blood pressure or breathing rate was established using midazolam-fentanyl-injection and isoflurane-inhalation. By placing an atraumatic clip to the Arteria hepatica and the portal vein, the upper lobes of the liver were completely drained from blood and remained entirely ischemic until the clip-removal (visual supervision). Upon restoration of blood supply, the blood pressure decreased about 20 – 40 mm Hg column for 15 – 20 minutes, but recovered soon thereafter. Mucous obstruction of airways could be observed rarely after 2 hours reperfusion. Animal body temperature was controlled rectally and maintained at 36.5°C with a red light heating lamp. Thus, constant conditions for all animal operations could be kept to ensure comparability of experiments.

4.5.1.1 Transaminases

The degree of transaminase activity in blood plasma provides information about the condition of damaged liver tissue. Figure 20 and Figure 21 indicate a rise in transaminase levels in the reperfusion period, but not after 1 hour of ischemia. Thus, hepatic injury starts with the restoration of the blood supply and is augmented with longer reperfusion times. Sham operated animals experienced the same treatment regarding anesthesia and preparation as IR-groups, apart from the clamping of the blood stream and the subsequent disconnection of the circulation. As transaminase activity of sham operated animals remain at baseline level, the elevation of ALT and AST concentrations in the blood plasma is solely caused by ischemia and reperfusion.
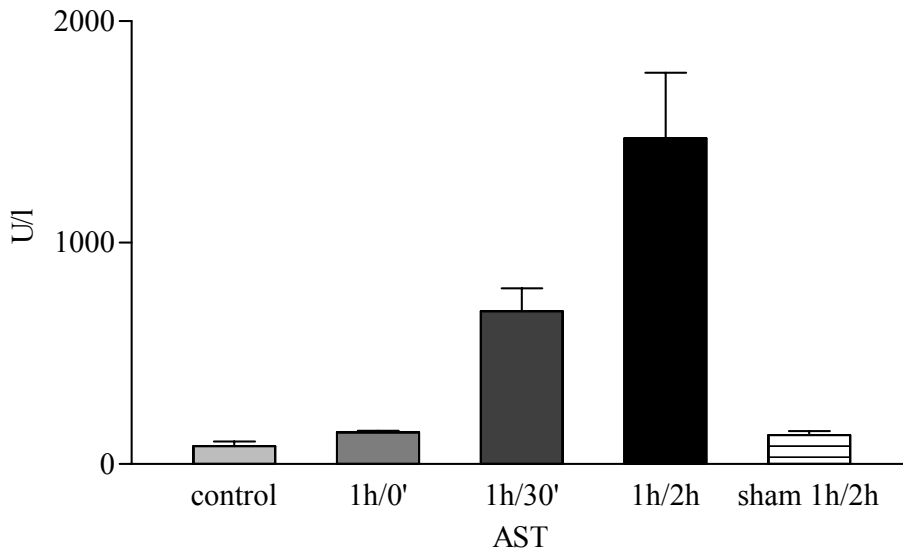
Figure 20 Impact of various reperfusion times on systemic AST levels. Measurement of AST activity
in heparinized blood plasma was performed as described in chapter 3.11.
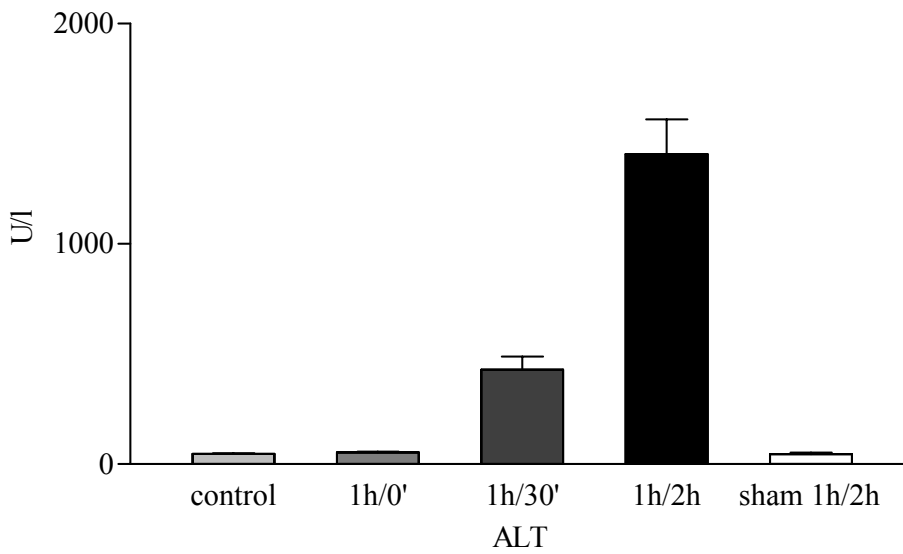
Figure 21 Impact of various reperfusion times on systemic ALT levels. Measurement of ALT activity
in heparinized blood plasma was performed as described in chapter 3.11.

4.5.1.2 NF-κB activity

We then conducted an EMSA analysis to check if NF-κB binding activity is increased after postischemic reperfusion. As depicted in Figure 22, NF-κB activity is upregulated upon reperfusion in comparison to untreated control liver tissue.
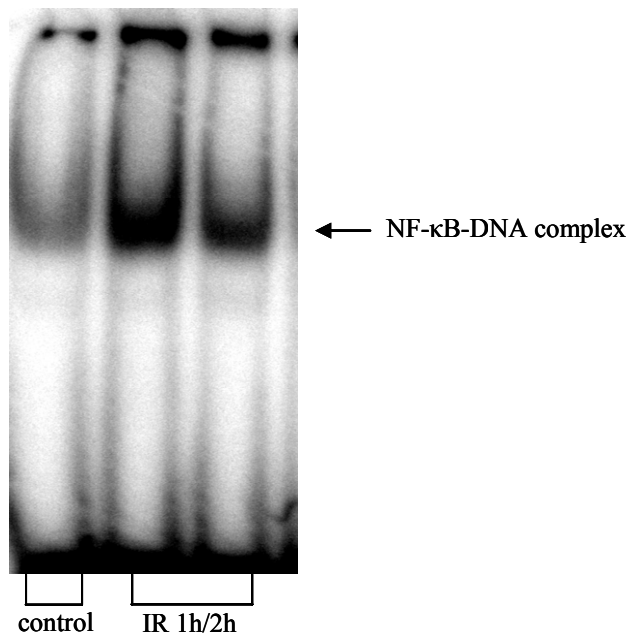
Figure 22 Ischemia/reperfusion induces NF-κB activity. Protein extraction and determination of NF-κB binding activity by electromobility shift assay (EMSA) was performed as described in section 3.8.

Interestingly, sham operated animals displayed an even further elevated NF-κB activation (Figure 23). As a distinct liver damage of sham operated animals is not evident (see transaminase activities Figure 20 and Figure 21), an increase of NF-κB activity might not be necessarily associated with early hepatic injury.
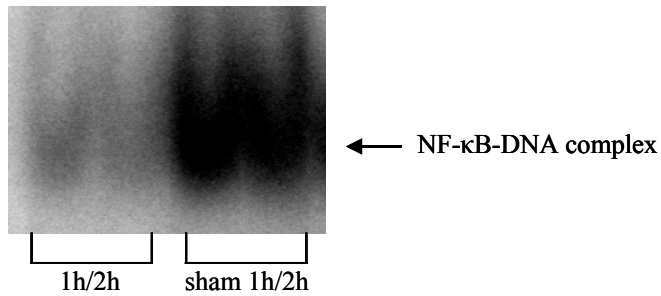
Figure 23 Sham operated animals show an enhanced NF-κB binding activity. Protein extraction and determination of NF-κB binding activity by electromobility shift assay (EMSA) was performed as described in section 3.8.

4.5.2 Influence of decoy nanoparticles on NF-κB activity

Figure 24 shows an EMSA analysis of animals treated with nanoparticles 15 minutes before the initiation of the ischemic period. Again, administration of decoy nanoparticles reduced NF-κB binding activity to baseline levels, leading to a significant difference compared to the scrambled decoy nanoparticle treated group.

NF-κB-DNA complex →

Ischemia/reperfusion 1h/2h		+	+	+	+
Decoy-NP			+		
scrambled Decoy-NP				+	
naked NP					+
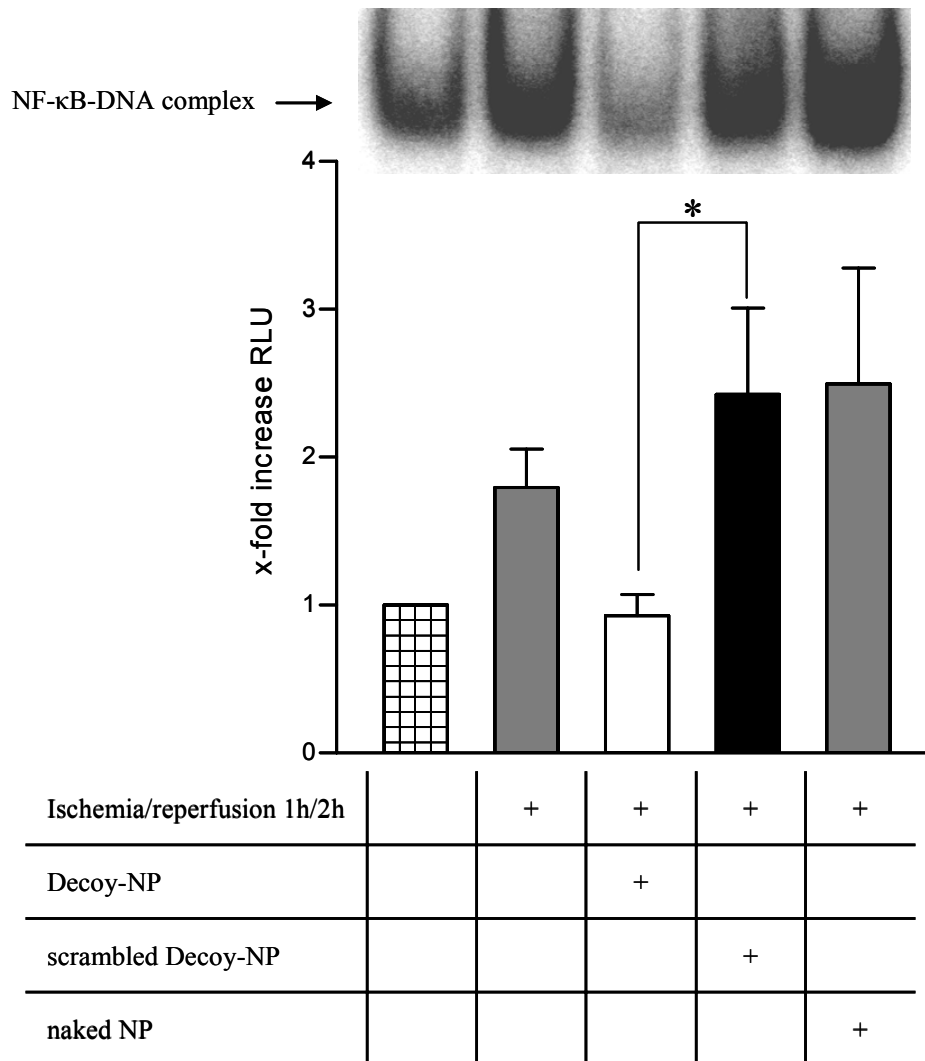
Figure 24 Administration of decoy nanoparticles reduces NF-κB binding activity induced by ischemia/reperfusion. Protein extraction and determination of NF-κB binding activity by electromobility shift assay (EMSA) was performed as described in section 3.8. All experiments were conducted three times. One representative EMSA blot is depicted above.

4.5.3 Influence of decoy nanoparticles on TNF-α

As we were able to show a significant reduction in NF-κB activation, we next addressed the issue of the impact on NF-κB mediated TNF-α signalling.

4.5.3.1 TNF-α mRNA expression

Real time RT-PCR was used to determine the changes in TNF-α mRNA expression. As depicted in Figure 25, application of decoy nanoparticles resulted in a significant reduction in expression levels versus scrambled decoy nanoparticle treated animals. This provides the evidence that employment of decoy nanoparticles interacts with NF-κB downstream signalling and interferes with inflammatory pathways in Kupffer cells. However, uptake of gelatin nanoparticles by Kupffer cells -irrespective of the load- seemed to cause an elevation in TNF-α expression per se, as mRNA levels are raised after nanoparticle injection.

		Ischemia/reperfusion 1h/2h	Decoy-NP	scrambled Decoy-NP
Ischemia/reperfusion 1h/2h		+	+	+
Decoy-NP			+	
scrambled Decoy-NP				+
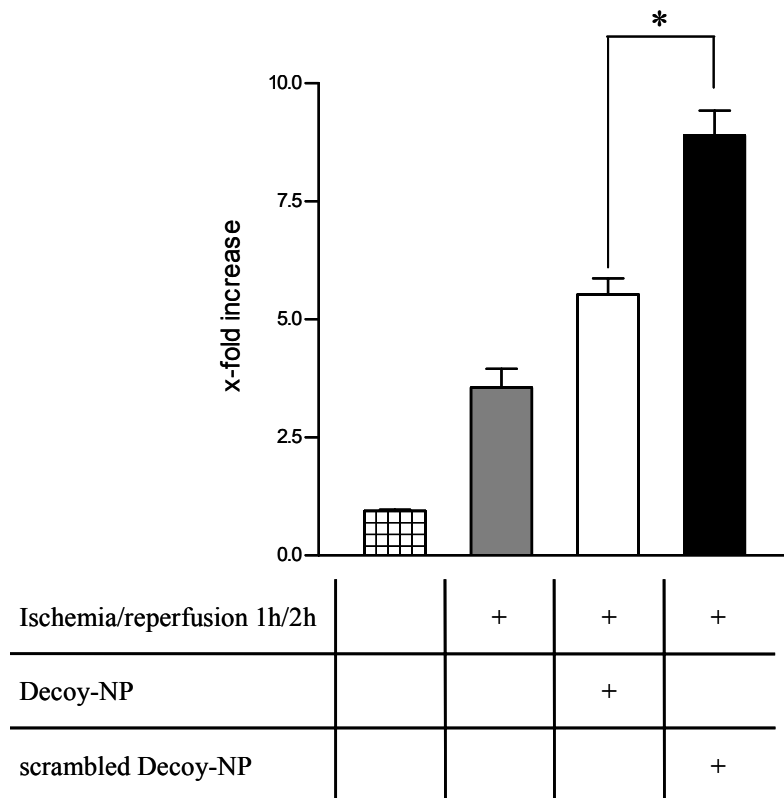
Figure 25 Administration of decoy nanoparticles diminishes IR induced TNF-α mRNA expression in comparison to the group that received scrambled decoy nanoparticles. RNA isolation and real time RT-PCR were performed as described in chapter 3.9. Experiments were conducted five times.

4.5.3.2 TNF-α release

Unlike systemic LPS challenge, the injury caused by hepatic ischemia and reperfusion is primary a local event. Therefore, an intervention in the liver with decoy nanoparticles should entail a change in TNF-α plasma levels. ELISA conducted with heparinized plasma samples indeed showed a decrease in systemic TNF-α release after decoy nanoparticle application in comparison to scrambled decoy nanoparticle treatment. However, no significant differences could be seen due to the large deviation of measurements.

		Ischemia/reperfusion 1h/2h		
Ischemia/reperfusion 1h/2h		+	+	+
Decoy-NP			+	
scrambled Decoy-NP				+
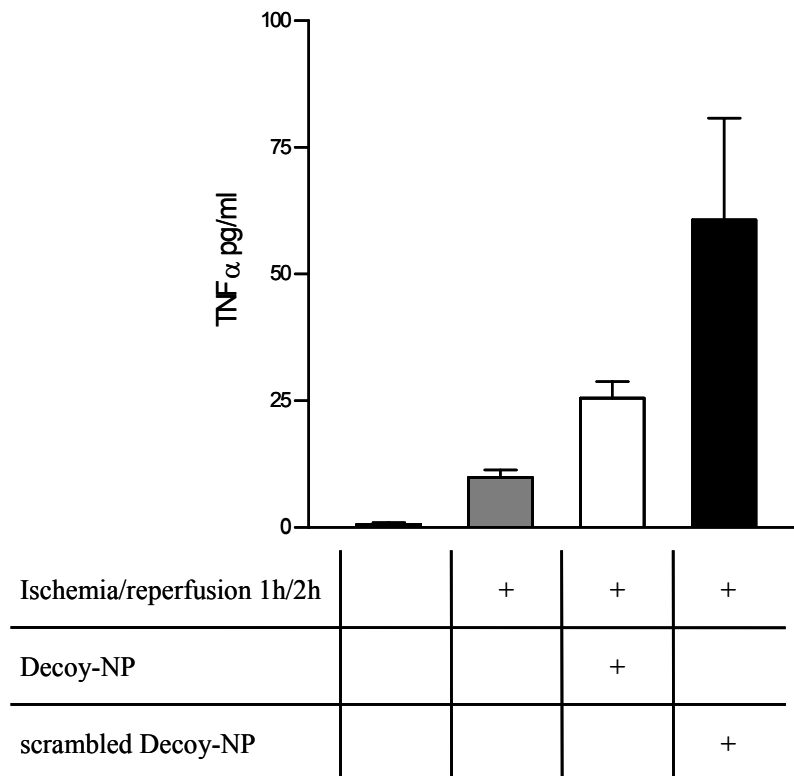
Figure 26 Decrease of systemic TNF-α cytokine levels by administration of decoy nanoparticles is statistically not significant. ELISA of heparinized blood plasma samples was performed as described in chapter 3.10. Experiments were conducted three times.

4.5.4 Influence on transaminase levels

The transaminases ALT and AST (GPT and GST respectively) are commonly accepted as markers for liver damage. Hence, we were interested in evaluating the change on liver damage by determining the impact of decoy nanoparticles on transaminase activities in blood samples. As shown in Figure 27 and Figure 28 respectively, transaminase levels were not affected by NF-κB-inhibition in Kupffer cells.

Ischemia/reperfusion 1h/2h	+	+	+	+
Decoy-NP		+		
scrambled Decoy-NP			+	
naked NP				+

Figure 27 Administration of nanoparticles does not affect systemic AST levels. Measurement of AST activity in heparinized blood plasma was performed as described in chapter 3.11.

Ischemia/reperfusion 1h/2h	+	+	+	+
Decoy-NP		+		
scrambled Decoy-NP			+	
naked NP				+

Figure 28 Administration of nanoparticles does not affect systemic ALT levels. Measurement of ALT activity in heparinized blood plasma was performed as described in chapter 3.11.

5 DISCUSSION

5.1 Targeting Kupffer cells with decoy nanoparticles

Kupffer cells are essential for inflammatory signalling in various hepatic disorders, such as ischemia/reperfusion injury, chronic 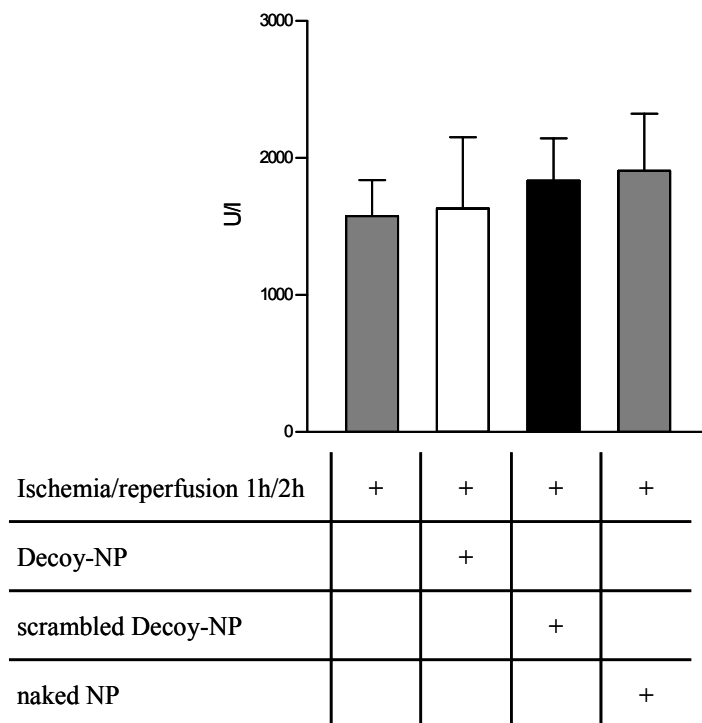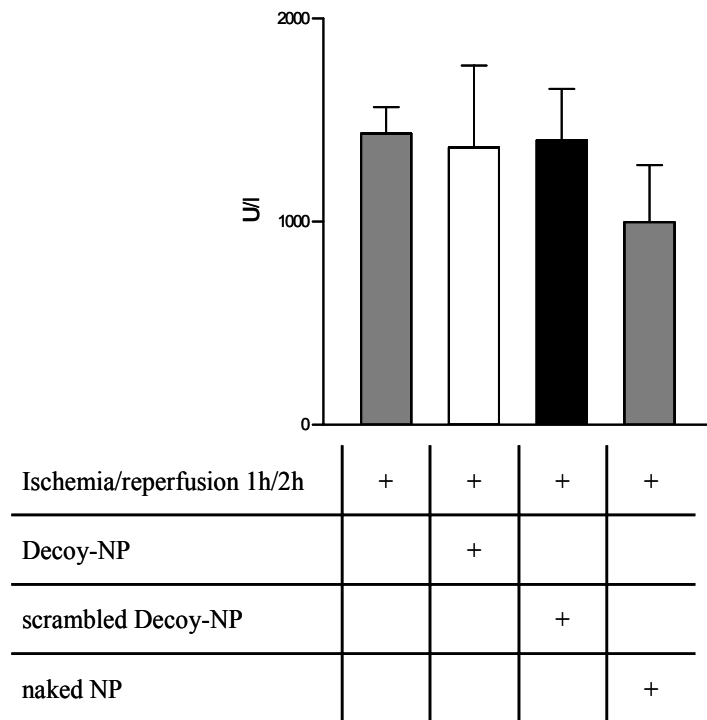alcoholic liver disease and LPS challenge (6;7;64). Cell culture experiments with isolated hepatocytes in fact revealed that LPS stimulation alone is not sufficient to induce hepatocyte apoptosis, unless either the supernatant of cultured Kupffer cells primed with LPS is added (68) or a co-culture system of hepatocytes and Kupffer cells is employed (67). Thus, inhibition of Kupffer cell activation is of great therapeutic interest. Along this line, the depletion of Kupffer cells by gadolinium chloride ameliorates the outcome of ischemia/reperfusion (76) or endotoxin challenge (66).

However, Kupffer cell depletion is not a clinically applicable method for various reasons: firstly, macrophage depletion by gadolinium chloride administration has to be initiated at least 24 h before the expected inflammatory injury, which is impractical in clinical situations. Secondly, as Kupffer cells are indispensable for a successful pathogen defense system, the complete loss of liver macrophages leads to a diminished immune response and enhanced susceptibility to pathogens (105;106). Therefore, finding ways for transient intervention into Kupffer cell mediated inflammatory pathways is a more promising approach. Utilizing NF-κB decoy loaded gelatin nanoparticles focuses directly on targeting Kupffer cell inflammatory signalling rather than whole cell destruction.

Activation of NF-κB in Kupffer cells is a central event in liver inflammation (17) and plays an important role in a multitude of pathological incidents, such as ischemia/reperfusion (38), chronic alcoholic liver disease (107), and LPS challenge (69;108). Several studies presented different approaches to interact with NF-κB signalling by using pharmacological drugs, natural products or by an overexpression of IκB (36;87;109). However, the special and dual role of NF-κB in the liver has to be taken into account. For example, p65-knockout mice die during embryogenesis due to massive hepatocyte apoptosis (31) and hepatocyte-specific NF-κB inhibition aggravates TNF-α provoked cell death (110). In contrast, downregulation of NF-κB

in isolated Kupffer cells leads to a decrease in the production of cytokines and adhesion molecules (27;108). Therefore, finding tools for an exclusive Kupffer cell specific NF-κB inhibition is of obvious importance.

To achieve such a selective Kupffer cell targeting, we used gelatin nanoparticles as a carrier for NF-κB inhibiting decoy oligonucleotides. In preliminary in vitro experiments we could prove that the decoy nanoparticles are taken up by isolated Kupffer cells as early as 15 minutes after the start of incubation. Moreover, we were able to confirm an explicit uptake of our nanoparticulate carrier in vivo by Kupffer cells and not by hepatocytes or other non-parenchymal cell types (Figure 8), providing the basis for Kupffer cell specific targeting. It is well known that upon intravenous administration, nanoparticles are rapidly cleared from the blood stream through phagocytosis, generally by macrophages of the reticuloendothelial system (RES) in liver and spleen (55). By labelling the decoy oligonucleotides with a fluorescent dye, we could demonstrate that the decoys are concomitantly transported to the Kupffer cells and are not detached under physiological in vivo conditions (Figure 9, Figure 10).

The groups of Ogushi and Higuchi respectively employed modified liposomal carriers (hemagglutinating virus of Japan (HVJ-) liposomes as well as mannosylated cationic liposomes) to deliver decoy oligonucleotides to Kupffer cells (69;70). Indeed, both groups detected a diminished inflammatory cytokine release upon LPS challenge. However, although liposomes are mainly taken up by Kupffer cells, the delivery to hepatocytes to some extent can not be ruled out, as liposomes display a flexible form and therefore have the ability to reach the parenchyma through the endothelial fenestrae (58;111;112). Solid, inflexible gelatin nanoparticles feature a defined particle size distribution in the range of 260 to 280 nm, and are thus too large to pass through between endothelial cells. Therefore, the uptake of gelatin nanoparticles by hepatocytes is almost impossible, as the parenchyma is not accessible for nanoparticulate constructs. In fact, we have shown that administration of decoy oligonucleotides encapsulated in DOTAP/DOPC liposomes results in a considerable loss of decoy oligonucleotides within the sinusoid along with an enhanced uptake by hepatocytes and endothelial cells in comparison to decoy loaded gelatin nanoparticles (Figure 11).

In summary, by utilizing gelatin nanoparticles we developed a new technical perspective to target Kupffer cells selectively with decoy oligonucleotides.

5.2 Impact of decoy nanoparticles on LPS challenge

Besides the specific uptake of our construct in Kupffer cells, it was pivotal that NF-κB decoy oligonucleotides carried by gelatin nanoparticles are in fact biologically active. To this end, RAW 264.7 macrophages were preincubated with NF-κB decoy nanoparticles before LPS challenge in vitro. Indeed, we found a reduction in LPS induced NF-κB DNA binding activity (Figure 14). We also examined the impact of decoy nanoparticles on LPS provoked activation of NF-κB in vivo and observed a likewise inhibition of NF-κB binding to DNA (Figure 16).

Translocation of NF-κB to the nucleus is a prerequisite for transcriptional function. Application of NF-κB decoy nanoparticle however seems to retain activated NF-κB in the cytoplasm, thereby preventing the access of the transcription factor to the nuclear promoter region (Figure 17). This data is in accordance with the work of Higuchi et al. 2005 (113), which showed an impeded translocation of NF-κB after NF-κB decoy administration in RAW 264.7 macrophages. However, there are also reports indicating that a cytoplasmatic distribution of AP-1 and NF-κB decoy oligonucleotides respectively might not be sufficient for the inhibition of the transcriptional activation of the respective transcription factors (114;115).

To confirm that our NF-κB decoy nanoparticles in fact inhibit NF-κB driven transcription, we measured the expression of the TNF-α gene, as Kupffer cells are the major source for the production and the release of TNF-α in the liver. The proinflammatory cytokine TNF-α represents a well recognized target of NF-κB activation, as the promoter region of the TNF-α gene possesses at least three binding sites for NF-κB (29). Administration of decoy nanoparticles prior to LPS challenge significantly decreased the hepatic TNF-α mRNA expression (Figure 18). This provides the proof of principle for our approach, as decoy nanoparticles interfere with NF-κB mediated downstream signalling in Kupffer cells.

Besides NF-κB, other transcription factors like activator protein 1 (AP-1), cAMP response element-binding protein (CREB) and early growth response factor 1 (Egr-1) possess matching binding sequences within the promoter region of the TNF-α gene (29). This could explain the observation that TNF-α mRNA expression is not fully abolished after decoy nanoparticle treatment in comparison to the complete reduction in NF-κB activity seen by EMSA analysis.

It has to be noted that TNF-α protein levels measured in blood plasma by ELISA remained unchanged (Figure 19). As intraportal LPS administration is a systemic challenge, other organs like spleen and kidney might contribute to the release of TNF-α (116). Thus, intervention with a Kupffer cell exclusive NF-κB blockade seems to have no influence on increased TNF-α levels, which originate from such a comprehensive stimulus. Moreover, the time interval between the application of the decoy nanoparticles and the actual measurement might be too short for detecting alterations in protein expression, as decoy treatment intervenes at the transcriptional stage. TNF-α levels however are not only regulated by transcription, but also by the release of preformed TNF-α.

In addition to a use as a mere experimental tool, application of decoy nanoparticles might emerge as a further option for the treatment of septic patients. NF-κB activity is markedly increased in patients with septic shock, and the degree of NF-κB activity correlates with the severity of the disease (117). Several approaches for inhibiting NF-κB and preventing inflammatory signalling cascades have been investigated so far. IκB as the regulatory switch for NF-κB translocation presents an apparent target and gene transfer strategy by the overexpression of IκB-α has been shown to have a beneficial effect (38). However, feasibility, safety and efficacy of this approach still remain key problems. Other NF-κB inhibitors include NSAIDs, small molecules and natural products (36;87;109). Yet miscellaneous secondary effects and non-specific interactions display limitations for this approach. Experiments with knock-out mice have tried to shed light on the role of NF-κB (118). These approaches, however, are time-consuming and difficult to accomplish and therefore not relevant for clinical applications.

Decoy nanoparticles in contrast have to be administered just a short time period beforehand, which presents a major advantage for their use. By the selective mode of inhibition of decoy oligonucleotides, unintended interactions with other proteins beside NF-κB can be excluded. Therefore, application of decoy nanoparticles in the initial period of sepsis could be considered as an additional alternative.

5.3 Impact of decoy nanoparticles on hepatic IR injury

Many proteins involved in aggravation of IR injury, like TNF-α, IL-1, CINC, ICAM-1 and others are strongly regulated by NF-κB mediated gene transcription. However, signalling cascades in hepatic ischemia/reperfusion are complex, and the role of NF-κB in this context is poorly understood.

Investigations on transgenic mice are the most common approach to elucidate the role of NF-κB in the liver and to provide a better understanding of hepatic NF-κB signalling. As mentioned above, p65 knock-out mice are not capable of surviving, emphasizing the importance of the RelA subunit (31). Mice deficient of the p50 subunit on the other hand show normal embryonic development with minor deficiencies in the immune response. If these mice are subjected to hepatic ischemia/reperfusion (119) or partial hepatectomy (120), no differences in the extent of damage can be found in comparison to wild-type animals. As IκBα is an important regulatory trigger, it provides an obvious target for inhibition of NF-κB by transfection with an overexpressed degradation-resistant form of IκBα. Using an adenoviral construct for delivery of this superrepressor to liver cells, Uesugi et al. (121) showed that chronic ethanol challenge, normally leading to NF-κB activation and thus to liver damage, could be diminished. This leads to the assumption, that overall inhibition of NF-κB in the liver is beneficial in this context. Hepatocyte-specific overexpression of a degradation-resistant form of IκBα however demonstrates a different view, as these animals are more susceptible to bacterial infections (122) and are more likely to undergo hepatocyte apoptosis after TNF-α treatment (110).

Another even more controversial picture is arising if the model of hepatic partial hepatectomy is applied. Iimuro et al. (34) detected an increased apoptosis of parenchymal cells after superrepressor delivery to the liver cells. Although most cells affected by this transfection were indeed hepatocytes, a small amount of Kupffer cells was targeted as well. This might explain the contradictory results presented by Chaisson et al. (110), as here hepatocyte-specific overexpression of IκBα is not connected with increased hepatocyte apoptosis or diminished proliferation upon partial hepatectomy. These data present first evidence for the importance of a cell-specific examination, as inhibition of NF-κB in Kupffer cells even to a minor extent seems to divert the hepatic fate to a different outcome.

IκBα is activated by the upstream kinase complex of IKK1 and 2 plus the regulatory unit NEMO. Therefore, deletion of these kinases results in an abolishment of NF-κB activation. As IKK1, IKK2 or NEMO constitutive knock-out mice die during embryogenesis or soon after birth (123), conditional hepatocyte-specific ablation of IKK2 or NEMO do not impair animal survival (88). Elimination of NEMO caused a complete block of NF-κB activation and increased hepatocyte apoptosis after TNF-α challenge. Hepatocyte IKK2 deletion however did not interfere with the degree of NF-κB activation. As a consequence, TNF-α treatment after IKK2 elimination could not initiate parenchymal cell death, but strikingly protected from hepatic ischemia/reperfusion injury. This prompts the assumption, that IKK2 has various functions in hepatocytes, depending on the mode of activation. A recent study by Dajani et al. (124) used an adenoviral construct to inhibit IKK2 in the liver. Here, the blockade of NF-κB activation by deletion of IKK2 led to diminished proinflammatory cytokine levels and increased survival upon LPS challenge. These results are in contrast to those discovered by Luedde et al. (88), who could not detect any improvement by the deletion of IKK2 in their conditional knock-out mouse. However, an adenoviral approach targets all liver cells, including Kupffer cells. Hence, downregulation of NF-κB in Kupffer cells might be the actual trigger, responsible for the reduced cytokine production in this model.

Another specific sight on the different roles of NF-κB in particular liver cell types is presented by Maeda et al. (125). Again, a mouse model with an IKK2 hepatocyte specific deletion was used to investigate diethylnitrosamine (DEN) induced

hepatocarcinogenesis. Surprisingly, inhibition of IKK2 in parenchymal cells (which actually means elimination of an antiapoptotic survival signal) promoted an increase in tumor size and progression, possibly by a compensatory proliferation of surviving hepatocytes. As an additional inhibition of IKK2 in Kupffer cells was able to reverse the carcinogenic effects, NF-κB in Kupffer cells seems to be responsible for releasing tumor-inducing agents that in turn prime hepatocytes for unregulated proliferation.

These data demonstrate that NF-κB regulation in the liver turns out to be a fine balanced process at multiple levels, which strongly depends on the cell type looked at. However, all obtained data were gained by the comparison of a NF-κB knock-out in all liver cells versus hepatocyte-specific deletion. Selective inhibition of NF-κB exclusively in Kupffer cells without involvement of hepatocytes has not been regarded so far due to technical impossibility. Herein, our study should provide new insights, as we favour a Kupffer cell targeting approach.

Recently, a report by the group of Lentsch (91) shed some light into the NF-κB controversy. In their model of warm IR, a slight decrease in the body temperature leading to hypothermia during ischemia caused an amelioration of hepatic injury. Amazingly, this correlated with an increase of NF-κB activity in whole liver homogenates. When normothermic controls were examined, the rise in NF-κB activity was diminished. Cell type specific differences could be evaluated by isolation of parenchymal and non-parenchymal cells. While NF-κB in hepatocytes was strongly activated during hypothermia and almost not present in normothermic controls, Kupffer cells showed an inverse activation scheme. Normothermic controls suffering from stronger liver damage showed a prominent NF-κB activation in Kupffer cells, but not in hepatocytes. Therefore it can be concluded, that macrophage NF-κB seems to be responsible for mediating IR injury. However, this study relies rather on isolated cells than on in vivo conditions, which allows only a limited transfer to the animal models.

Ischemia/reperfusion causes a time-dependent rise of ALT and AST levels in blood plasma (Figure 20), as the hepatocyte cell membrane gets more porous upon liver damage. Inhibition of NF-κB by application of decoy nanoparticles however did not

cause a reduction in the transaminase release (Figure 27). These results might indicate that upregulation of NF-κB activity in Kupffer cells is not necessarily linked to an acutely higher damage.

This is in accordance with our EMSA analysis of sham-operated animals, as increased NF-κB activation is found there in line with low transaminase activity at baseline levels (Figure 23). This increase might result from upregulation of protective NF-κB in hepatocytes due to anesthesia and surgery alone, counteracting a potential threat. Not many reports on the field of warm IR actually determine the degree of NF-κB activation in sham-operated controls, indicating that the interpretation of the obtained results might be problematic. Interestingly, few groups also showed a remarkable increase in sham NF-κB activity (87;91;126). Yet, many studies claimed a connection between elevated NF-κB activity and raised transaminase levels. However, reports that implicated a detrimental role of NF-κB in liver ischemia/reperfusion injury, acquired data by applying different medication that reduced the hepatic damage (86;127-129). Along this line, a concomitant reduction in NF-κB activity could be seen. A cell type specific examination and reflection however was hardly conducted. This could lead to misinterpretations, as the source of the increase in NF-κB activity can not be determined. A rise in NF-κB activity in hepatocytes is thought to protect the liver cells from external harmful events and signals. If the NF-κB inhibition is mainly achieved in Kupffer cells, then less damaging cytokines are released, thus diminishing the need of hepatocytes to compensate the damaging stimulus by activating NF-κB. This might prompt the interpretation that diminished NF-κB levels in the entire liver correlate with a protective effect and diminished transaminase levels. Above all, every pharmacological intervention could also primarily result in attenuation of ROS production. Any detected reduction of NF-κB levels therefore are just secondary effects among others, as decreased ROS release affects multiple different signalling cascades besides NF-κB.

Hence, these controversial data can only be clarified by the use of an exclusive, well-defined inhibitor that is able to interact with NF-κB without affecting other proteins.

We were able to demonstrate that NF-κB decoy oligonucleotides interact specifically with NF-κB (Figure 13), as decoy oligonucleotides mixed with active NF-κB prohibits binding of the transcription factor to other consensus-sequence containing DNA-strands. Administration of decoy nanoparticles prior to ischemia reduced NF-κB binding activity as well as TNF-α mRNA expression. It has to be noted that the injection of gelatin nanoparticles itselve (loaded or unloaded) seems to provoke an increase in TNF-α mRNA expression and release. The nanoparticles are probably taken up by Kupffer cells through phagocytosis. Challenging Kupffer cells with nanoparticles causes an inflammatory response, in fact by the ingestion procedure itself (54). Production of TNF-α is a common response by Kupffer cells after phagocytosis of external material (like bacteria), as secretion of cytokines is a major mechanism in host defense. This might explain the increased TNF-α levels after nanoparticle administration, as the Kupffer cells react on this stimulation the way they are proposed to do.

As most reports rely on whole liver homogenates, changes of NF-κB levels in Kupffer cells could remain undetected due to the predominant mass of hepatocytes. Unfortunately, we were not able to illuminate the cell type, which is prompted by IR to enhance NF-κB activity. However, our results reveal that a selective inhibition in Kupffer cells diminishes NF-κB levels of the entire liver. Hence, it can be concluded that either Kupffer cells are the primary source of NF-κB in this setting, or that hepatocyte derived NF-κB is only upregulated in response to NF-κB dependent signals originated from Kupffer cells.

5.4 Outlook

An abolishment of NF-κB activity in the liver is expected to massively change hepatic transcription. And indeed, we were able to show a significant reduction in TNF-α mRNA expression levels. To screen other possible targets, a genechip analysis is currently conducted in cooperation with the Laboratory for Functional Genome Analysis (Lafuga, Großhadern, Germany). Using the whole rat genome

GeneChip 230 2.0 by Affymetrix®, the obtained results should provide interesting insights into the altered gene expression pattern by the inhibition of NF-κB in Kupffer cells during hepatic ischemia/reperfusion.

Besides potential therapeutical implications in inflammatory liver processes, decoy nanoparticles are a helpful tool to decipher the pleiotropic and cell specific role of NF-κB and its impact on the entire hepatic transcellular signalling system. For instance, an application of decoy nanoparticles promises to be of special interest in diethylnitrosamine (DEN) induced hepatocarcinogenesis, where NF-κB is transiently elevated in Kupffer cells (125;130).

In addition to sepsis, elevated NF-κB levels in Kupffer cells are also found during alcoholic hepatitis (131) and liver fibrosis (132), which might present further attractive targets for an intervention with NF-κB decoy nanoparticles.

During liver transplantation proceedings, the extracted organ is stored at a temperature of 4°C throughout the transportation interval in order to reduce the metabolic rate and to minimize tissue damage. After this cold ischemic period, non-parenchymal cells like Kupffer cells are thought to be activated to a larger extent than in our model of warm ischemia/reperfusion (71). Hence, the use of Kupffer cell targeting decoy nanoparticles should be of great interest in this context. Liver transplantations can be simulated by applying the model of the isolated perfused rat liver, and further investigations are currently conducted in our group to evaluate the impact of decoy nanoparticles on reperfusion injury provoked by prolonged cold ischemia. In addition, working in an isolated model with a blood free environment provides the advantage that interaction of liver cells can be analysed exclusively, without the involvement of non-hepatic cell types.

6 SUMMARY

In this present study we established a new approach to target Kupffer cells with decoy oligonucleotides.

Initially, we validated that gelatin nanoparticles are an appropriate carrier to deliver NF-κB decoy oligonucleotides to the resident liver macrophages. Distribution studies demonstrated that decoy nanoparticles are taken up selectively into Kupffer cells upon intraportal injection, whereas hepatocytes remained completely unaffected.

The proof of principle was provided in a LPS model. The LPS induced upregulation of NF-κB activity could be diminished after administration of decoy nanoparticles. Furthermore, the subsequent increase in TNF-α mRNA expression was also significantly reduced, thus proving the feasibility of our approach.

After establishing a rat model of hepatic partial warm ischemia/reperfusion, we were able to show that an elevation of NF-κB activity caused by ischemia/reperfusion was strongly reduced by the application of decoy nanoparticles. Concomitantly, a decrease in TNF-α mRNA levels could be seen. A following Gene Chip analysis should provide additional targets affected by this intervention.

In summary, intraportal injection of decoy nanoparticles prior to LPS challenge or hepatic ischemia/reperfusion abolished induction of NF-κB as well as a subsequent TNF-α mRNA expression (Figure 29). Kupffer cells were the only liver cells affected by administration of decoy nanoparticles. Hence, the downregulation of NF-κB in the entire liver has to originate from the resident liver macrophages, whereas hepatocytes are only secondary involved in this effect. The overall changes in liver signalling provoked by this selective NF-κB inhibition remain to be further investigated. This will help to decipher the impact of NF-κB on hepatic ischemia/reperfusion injury, which is still elusive and not at all clarified.
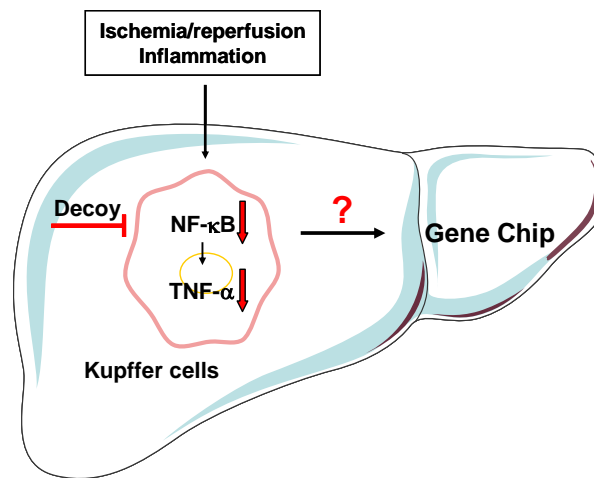
Figure 29   Summary

Alex Lentsch (133) wrote a comment in *Hepatology* on the work of Luedde et al. (88) concerning the role of IKK2 in hepatic ischemia/reperfusion. He concluded that "NF-κB in Kupffer cells is presumed to be largely responsible for the wave of proinflammatory cytokines released, … although this contention has never been rigorously tested." In this work we present NF-κB decoy nanoparticles as a capable tool, that enables us to interfere selectively with NF-κB in Kupffer cells and that gives us the opportunity, to further elucidate the role of this transcription factor in various settings like ischemia/reperfusion injury or LPS/N-galactosamine induced liver injury.

7 REFERENCES

1. Imose,M., Nagaki,M., Naiki,T., Osawa,Y., Brenner,D.A., Asano,T., Hayashi,H., Kato,T. and Moriwaki,H. (2003) Inhibition of nuclear factor kappaB and phosphatidylinositol 3-kinase/Akt is essential for massive hepatocyte apoptosis induced by tumor necrosis factor alpha in mice. *Liver Int.*, **23**, 386-396.

2. Yang,L., Magness,S.T., Bataller,R., Rippe,R.A. and Brenner,D.A. (2005) NF-kappaB activation in Kupffer cells after partial hepatectomy. *Am. J. Physiol Gastrointest. Liver Physiol*, **289**, G530-G538.

3. Takahashi,Y., Ganster,R.W., Gambotto,A., Shao,L., Kaizu,T., Wu,T., Yagnik,G.P., Nakao,A., Tsoulfas,G., Ishikawa,T. *et al.* (2002) Role of NF-kappaB on liver cold ischemia-reperfusion injury. *Am. J. Physiol Gastrointest. Liver Physiol*, **283**, G1175-G1184.

4. Malarkey,D.E., Johnson,K., Ryan,L., Boorman,G. and Maronpot,R.R. (2005) New insights into functional aspects of liver morphology. *Toxicol. Pathol.*, **33**, 27-34.

5. Tsukamoto,H. (2002) Redox regulation of cytokine expression in Kupffer cells. *Antioxid. Redox. Signal.*, **4**, 741-748.

6. Decker,K. (1990) Biologically active products of stimulated liver macrophages (Kupffer cells). *Eur. J. Biochem.*, **192**, 245-261.

7. Bilzer,M., Roggel,F. and Gerbes,A.L. (2006) Role of Kupffer cells in host defense and liver disease. *Liver Int.*, **26**, 1175-1186.

8. Schwabe,R.F. and Brenner,D.A. (2006) Mechanisms of Liver Injury. I. TNF-alpha-induced liver injury: role of IKK, JNK, and ROS pathways. *Am. J. Physiol Gastrointest. Liver Physiol*, **290**, G583-G589.

9. Ding,W.X. and Yin,X.M. (2004) Dissection of the multiple mechanisms of TNF-alpha-induced apoptosis in liver injury. *J. Cell Mol. Med.*, **8**, 445-454.

10. Naito,M., Hasegawa,G., Ebe,Y. and Yamamoto,T. (2004) Differentiation and function of Kupffer cells. *Med. Electron Microsc.*, **37**, 16-28.

11. Kolios,G., Valatas,V. and Kouroumalis,E. (2006) Role of Kupffer cells in the pathogenesis of liver disease. *World J. Gastroenterol.*, **12**, 7413-7420.

12. Abshagen,K., Eipel,C., Kalff,J.C., Menger,M.D. and Vollmar,B. (2007) Loss of NF-{kappa}B activation in Kupffer cell-depleted mice impairs liver regeneration after partial hepatectomy. *Am. J. Physiol Gastrointest. Liver Physiol.*, **292**, G1570-G1577.

13. Rentsch,M., Puellmann,K., Sirek,S., Iesalnieks,I., Kienle,K., Mueller,T., Bolder,U., Geissler,E., Jauch,K.W. and Beham,A. (2005) Benefit of Kupffer cell modulation with glycine versus Kupffer cell depletion after liver transplantation in the rat: effects on postischemic reperfusion injury, apoptotic cell death graft regeneration and survival. *Transpl. Int.*, **18**, 1079-1089.

14. Frankenberg,M.V., Weimann,J., Fritz,S., Fiedler,J., Mehrabi,A., Buchler,M.W. and Kraus,T.W. (2005) Gadolinium chloride-induced improvement of postischemic hepatic perfusion after warm ischemia is associated with reduced hepatic endothelin secretion. *Transpl. Int.*, **18**, 429-436.

15. Suzuki,S., Nakamura,S., Serizawa,A., Sakaguchi,T., Konno,H., Muro,H., Kosugi,I. and Baba,S. (1996) Role of Kupffer cells and the spleen in modulation of endotoxin-induced liver injury after partial hepatectomy. *Hepatology*, **24**, 219-225.

16. Parker,G.A. and Picut,C.A. (2005) Liver immunobiology. *Toxicol. Pathol.*, **33**, 52-62.

17. Liu,S.F. and Malik,A.B. (2006) NF-kappa B activation as a pathological mechanism of septic shock and inflammation. *Am. J. Physiol Lung Cell Mol. Physiol*, **290**, L622-L645.

18. Baldwin,A.S., Jr. (1996) The NF-kappa B and I kappa B proteins: new discoveries and insights. *Annu. Rev. Immunol.*, **14**, 649-683.

19. Kucharczak,J., Simmons,M.J., Fan,Y. and Gelinas,C. (2003) To be, or not to be: NF-kappaB is the answer--role of Rel/NF-kappaB in the regulation of apoptosis. *Oncogene*, **22**, 8961-8982.

20. Pahl,H.L. (1999) Activators and target genes of Rel/NF-kappaB transcription factors. *Oncogene*, **18**, 6853-6866.

21. Wang,T., Zhang,X. and Li,J.J. (2002) The role of NF-kappaB in the regulation of cell stress responses. *Int. Immunopharmacol.*, **2**, 1509-1520.

22. Luedde,T. and Trautwein,C. (2006) Intracellular survival pathways in the liver. *Liver Int.*, **26**, 1163-1174.

23. Luo,J.L., Kamata,H. and Karin,M. (2005) IKK/NF-kappaB signaling: balancing life and death--a new approach to cancer therapy. *J. Clin. Invest*, **115**, 2625-2632.

24. Zwacka,R.M., Zhang,Y., Zhou,W., Halldorson,J. and Engelhardt,J.F. (1998) Ischemia/reperfusion injury in the liver of BALB/c mice activates AP-1 and nuclear factor kappaB independently of IkappaB degradation. *Hepatology*, **28**, 1022-1030.

25. Kumar,A., Takada,Y., Boriek,A.M. and Aggarwal,B.B. (2004) Nuclear factor-kappaB: its role in health and disease. *J. Mol. Med.*, **82**, 434-448.

26. Aggarwal,B.B. (2003) Signalling pathways of the TNF superfamily: a double-edged sword. *Nat. Rev. Immunol.*, **3**, 745-756.

27. Wheeler,M.D., Yamashina,S., Froh,M., Rusyn,I. and Thurman,R.G. (2001) Adenoviral gene delivery can inactivate Kupffer cells: role of oxidants in NF-kappaB activation and cytokine production. *J. Leukoc. Biol.*, **69**, 622-630.

28. Fox,E.S., Cantrell,C.H. and Leingang,K.A. (1996) Inhibition of the Kupffer cell inflammatory response by acute ethanol: NF-kappa B activation and subsequent cytokine production. *Biochem. Biophys. Res. Commun.*, **225**, 134-140.

29. Lee,Y.W. and Hirani,A.A. (2006) Role of interleukin-4 in atherosclerosis. *Arch. Pharm. Res.*, **29**, 1-15.

30. Liu,H., Lo,C.R. and Czaja,M.J. (2002) NF-kappaB inhibition sensitizes hepatocytes to TNF-induced apoptosis through a sustained activation of JNK and c-Jun. *Hepatology*, **35**, 772-778.

31. Beg,A.A., Sha,W.C., Bronson,R.T., Ghosh,S. and Baltimore,D. (1995) Embryonic Lethality and Liver Degeneration in Mice Lacking the Rela Component of Nf-Kappa-B. *Nature*, **376**, 167-170.

32. Selzner,N., Selzner,M., Odermatt,B., Tian,Y., Van Rooijen,N. and Clavien,P.A. (2003) ICAM-1 triggers liver regeneration through leukocyte recruitment and Kupffer cell-dependent release of TNF-alpha/IL-6 in mice. *Gastroenterology*, **124**, 692-700.

33. Kirillova,I., Chaisson,M. and Fausto,N. (1999) Tumor necrosis factor induces DNA replication in hepatic cells through nuclear factor kappaB activation. *Cell Growth Differ.*, **10**, 819-828.

34. Iimuro,Y., Nishiura,T., Hellerbrand,C., Behrns,K.E., Schoonhoven,R., Grisham,J.W. and Brenner,D.A. (1998) NFkappaB prevents apoptosis and liver dysfunction during liver regeneration. *J. Clin. Invest*, **101**, 802-811.

35. Heyninck,K., Wullaert,A. and Beyaert,R. (2003) Nuclear factor-kappa B plays a central role in tumour necrosis factor-mediated liver disease. *Biochem. Pharmacol.*, **66**, 1409-1415.

36. Pande,V. and Ramos,M.J. (2005) NF-kappaB in human disease: current inhibitors and prospects for de novo structure based design of inhibitors. *Curr. Med. Chem.*, **12**, 357-374.

37. Epinat,J.C. and Gilmore,T.D. (1999) Diverse agents act at multiple levels to inhibit the Rel/NF-kappaB signal transduction pathway. *Oncogene*, **18**, 6896-6909.

38. Suetsugu,H., Iimuro,Y., Uehara,T., Nishio,T., Harada,N., Yoshida,M., Hatano,E., Son,G., Fujimoto,J. and Yamaoka,Y. (2005) Nuclear factor {kappa}B inactivation in the rat liver ameliorates short term total warm ischaemia/reperfusion injury. *Gut*, **54**, 835-842.

39. Strnad,J. and Burke,J.R. (2007) IkappaB kinase inhibitors for treating autoimmune and inflammatory disorders: potential and challenges. *Trends Pharmacol. Sci.*, **28**, 142-148.

40. Luedde,T., Beraza,N., Kotsikoris,V., van,L.G., Nenci,A., De,V.R., Roskams,T., Trautwein,C. and Pasparakis,M. (2007) Deletion of NEMO/IKKgamma in liver parenchymal cells causes steatohepatitis and hepatocellular carcinoma. *Cancer Cell*, **11**, 119-132.

41. Mann,M.J. and Dzau,V.J. (2000) Therapeutic applications of transcription factor decoy oligonucleotides. *J. Clin. Invest*, **106**, 1071-1075.

42. Morishita,R., Tomita,N., Kaneda,Y. and Ogihara,T. (2004) Molecular therapy to inhibit NFkappaB activation by transcription factor decoy oligonucleotides. *Curr. Opin. Pharmacol.*, **4**, 139-146.

43. Isomura,I. and Morita,A. (2006) Regulation of NF-kappa B Signaling by Decoy Oligodeoxynucleotides. *Microbiol. Immunol.*, **50**, 559-563.

44. Cao,C.C., Ding,X.Q., Ou,Z.L., Liu,C.F., Li,P., Wang,L. and Zhu,C.F. (2004) In vivo transfection of NF-kappaB decoy oligodeoxynucleotides attenuate renal ischemia/reperfusion injury in rats. *Kidney Int.*, **65**, 834-845.

45. Kawamura,I., Morishita,R., Tsujimoto,S., Manda,T., Tomoi,M., Tomita,N., Goto,T., Ogihara,T. and Kaneda,Y. (2001) Intravenous injection of oligodeoxynucleotides to the NF-kappaB binding site inhibits hepatic metastasis of M5076 reticulosarcoma in mice. *Gene Ther.*, **8**, 905-912.

46. Ueno,T., Sawa,Y., Kitagawa-Sakakida,S., Nishimura,M., Morishita,R., Kaneda,Y., Kohmura,E., Yoshimine,T. and Matsuda,H. (2001) Nuclear factor-kappa B decoy attenuates neuronal damage after global brain ischemia: a future strategy for brain protection during circulatory arrest. *J. Thorac. Cardiovasc. Surg.*, **122**, 720-727.

47. Kawakami,S., Wong,J., Sato,A., Hattori,Y., Yamashita,F. and Hashida,M. (2000) Biodistribution characteristics of mannosylated, fucosylated, and galactosylated liposomes in mice. *Biochim. Biophys. Acta*, **1524**, 258-265.

48. Garcia-Chaumont,C., Seksek,O., Grzybowska,J., Borowski,E. and Bolard,J. (2000) Delivery systems for antisense oligonucleotides. *Pharmacology & Therapeutics*, **87**, 255-277.

49. Ponnappa,B.C. and Israel,Y. (2002) Targeting Kupffer cells with antisense oligonucleotides. *Frontiers in Bioscience*, **7**, E223-E233.

50. Yoshida,M., Yamamoto,N., Uehara,T., Terao,R., Nitta,T., Harada,N., Hatano,E., Iimuro,Y. and Yamaoka,Y. (2002) Kupffer cell targeting by intraportal injection of the HVJ cationic liposome. *Eur. Surg. Res.*, **34**, 251-259.

51. Bijsterbosch,M.K., Manoharan,M., Dorland,R., Waarlo,I.H., Biessen,E.A. and van Berkel,T.J. (2001) Delivery of cholesteryl-conjugated phosphorothioate oligodeoxynucleotides to Kupffer cells by lactosylated low-density lipoprotein. *Biochem. Pharmacol.*, **62**, 627-633.

52. Melgert,B.N., Weert,B., Schellekens,H., Meijer,D.K. and Poelstra,K. (2003) The pharmacokinetic and biological activity profile of dexamethasone targeted to sinusoidal endothelial and Kupffer cells. *J. Drug Target*, **11**, 1-10.

53. Crettaz,J., Berraondo,P., Mauleon,I., Ochoa,L., Shankar,V., Barajas,M., van,R.N., Kochanek,S., Qian,C., Prieto,J. *et al.* (2006) Intrahepatic injection of adenovirus reduces inflammation and increases gene transfer and therapeutic effect in mice. *Hepatology*, **44**, 623-632.

54. Fernandez-Urrusuno,R., Fattal,E., Rodrigues,J.M., Jr., Feger,J., Bedossa,P. and Couvreur,P. (1996) Effect of polymeric nanoparticle administration on the clearance activity of the mononuclear phagocyte system in mice. *J. Biomed. Mater. Res.*, **31**, 401-408.

55. Kommareddy,S. and Amiji,M. (2006) Biodistribution and pharmacokinetic analysis of long-circulating thiolated gelatin nanoparticles following systemic administration in breast cancer-bearing mice. *J. Pharm. Sci.*, **96**, 397-407.

56. Soppimath,K.S., Aminabhavi,T.M., Kulkarni,A.R. and Rudzinski,W.E. (2001) Biodegradable polymeric nanoparticles as drug delivery devices. *J. Control Release*, **70**, 1-20.

57. Lambert,G., Fattal,E. and Couvreur,P. (2001) Nanoparticulate systems for the delivery of antisense oligonucleotides. *Adv. Drug Deliv. Rev.*, **47**, 99-112.

58. Romero,E.L., Morilla,M.J., Regts,J., Koning,G.A. and Scherphof,G.L. (1999) On the mechanism of hepatic transendothelial passage of large liposomes. *FEBS Lett.*, **448**, 193-196.

59. Marty,J.J., Oppenheim,R.C. and Speiser,P. (1978) Nanoparticles - New Colloidal Drug Delivery System. *Pharmaceutica Acta Helvetiae*, **53**, 17-23.

60. Coester,C.J., Langer,K., von Briesen,H. and Kreuter,J. (2000) Gelatin nanoparticles by two step desolvation - a new preparation method, surface modifications and cell uptake. *Journal of Microencapsulation*, **17**, 187-193.

61. Zillies,J. and Coester,C. (2005) Evaluating gelatin based nanoparticles as a carrier system for double stranded oligonucleotides. *J. Pharm. Pharm. Sci.*, **7**, 17-21.

62. Zwiorek,K., Kloeckner,J., Wagner,E. and Coester,C. (2005) Gelatin nanoparticles as a new and simple gene delivery system. *J. Pharm. Pharm. Sci.*, **7**, 22-28.

63. Coester,C., Nayyar,P. and Samuel,J. (2006) In vitro uptake of gelatin nanoparticles by murine dendritic cells and their intracellular localisation. *Eur. J. Pharm. Biopharm.*, **62**, 306-314.

64. Su,G.L. (2002) Lipopolysaccharides in liver injury: molecular mechanisms of Kupffer cell activation. *Am. J. Physiol Gastrointest. Liver Physiol*, **283**, G256-G265.

65. Liu,S.F., Ye,X. and Malik,A.B. (1999) Inhibition of NF-kappaB activation by pyrrolidine dithiocarbamate prevents In vivo expression of proinflammatory genes. *Circulation*, **100**, 1330-1337.

66. Vollmar,B., Ruttinger,D., Wanner,G.A., Leiderer,R. and Menger,M.D. (1996) Modulation of kupffer cell activity by gadolinium chloride in endotoxemic rats. *Shock*, **6**, 434-441.

67. Milosevic,N., Schawalder,H. and Maier,P. (1999) Kupffer cell-mediated differential down-regulation of cytochrome P450 metabolism in rat hepatocytes. *Eur. J. Pharmacol.*, **368**, 75-87.

68. Hamada,E., Nishida,T., Uchiyama,Y., Nakamura,J., Isahara,K., Kazuo,H., Huang,T.P., Momoi,T., Ito,T. and Matsuda,H. (1999) Activation of Kupffer cells and caspase-3 involved in rat hepatocyte apoptosis induced by endotoxin. *J. Hepatol.*, **30**, 807-818.

69. Ogushi,I., Iimuro,Y., Seki,E., Son,G., Hirano,T., Hada,T., Tsutsui,H., Nakanishi,K., Morishita,R., Kaneda,Y. *et al.* (2003) Nuclear factor kappa B decoy oligodeoxynucleotides prevent endotoxin-induced fatal liver failure in a murine model. *Hepatology*, **38**, 335-344.

70. Higuchi,Y., Kawakami,S., Oka,M., Yabe,Y., Yamashita,F. and Hashida,M. (2006) Intravenous administration of mannosylated cationic liposome/NFkappaB decoy complexes effectively prevent LPS-induced cytokine production in a murine liver failure model. *FEBS Lett.*, **580**, 3706-3714.

71. Ikeda,T., Yanaga,K., Kishikawa,K., Kakizoe,S., Shimada,M. and Sugimachi,K. (1992) Ischemic injury in liver transplantation: difference in injury sites between warm and cold ischemia in rats. *Hepatology*, **16**, 454-461.

72. Bilzer,M. and Gerbes,A.L. (2000) Preservation injury of the liver: mechanisms and novel therapeutic strategies. *J. Hepatol.*, **32**, 508-515.

73. Teoh,N.C. and Farrell,G.C. (2003) Hepatic ischemia reperfusion injury: Pathogenic mechanisms and basis for hepatoprotection. *J. Gastroenterol. Hepatol.*, **18**, 891-902.

74. Jaeschke,H. (2003) Molecular mechanisms of hepatic ischemia-reperfusion injury and preconditioning. *Am. J. Physiol Gastrointest. Liver Physiol*, **284**, G15-G26.

75. Serracino-Inglott,F., Habib,N.A. and Mathie,R.T. (2001) Hepatic ischemia-reperfusion injury. *Am. J. Surg.*, **181**, 160-166.

76. Shiratori,Y., Kiriyama,H., Fukushi,Y., Nagura,T., Takada,H., Hai,K. and Kamii,K. (1994) Modulation of ischemia-reperfusion-induced hepatic injury by Kupffer cells. *Dig. Dis. Sci.*, **39**, 1265-1272.

77. Hisama,N., Yamaguchi,Y., Ishiko,T., Miyanari,N., Ichiguchi,O., Goto,M., Mori,K., Watanabe,K., Kawamura,K., Tsurufuji,S. *et al.* (1996) Kupffer cell

production of cytokine-induced neutrophil chemoattractant following ischemia/reperfusion injury in rats. *Hepatology*, **24**, 1193-1198.

78. Mosher,B., Dean,R., Harkema,J., Remick,D., Palma,J. and Crockett,E. (2001) Inhibition of Kupffer cells reduced CXC chemokine production and liver injury. *J. Surg. Res.*, **99**, 201-210.

79. Giakoustidis,D.E., Iliadis,S., Tsantilas,D., Papageorgiou,G., Kontos,N., Kostopoulou,E., Botsoglou,N.A., Gerasimidis,T. and Dimitriadou,A. (2003) Blockade of Kupffer cells by gadolinium chloride reduces lipid peroxidation and protects liver from ischemia/reperfusion injury. *Hepatogastroenterology*, **50**, 1587-1592.

80. Meijer,C., Wiezer,M.J., Diehl,A.M., Schouten,H.J., Schouten,H.J., Meijer,S., Van Rooijen,N., van Lambalgen,A.A., Dijkstra,C.D. and van Leeuwen,P.A. (2000) Kupffer cell depletion by CI2MDP-liposomes alters hepatic cytokine expression and delays liver regeneration after partial hepatectomy. *Liver*, **20**, 66-77.

81. Watanabe,M., Chijiiwa,K., Kameoka,N., Yamaguchi,K., Kuroki,S. and Tanaka,M. (2000) Gadolinium pretreatment decreases survival and impairs liver regeneration after partial hepatectomy under ischemia/reperfusion in rats. *Surgery*, **127**, 456-463.

82. Bell,F.P., Essani,N.A., Manning,A.M. and Jaeschke,H. (1997) Ischemia-reperfusion activates the nuclear transcription factor NF-kappa B and upregulates messenger RNA synthesis of adhesion molecules in the liver in vivo. *Hepatology Research*, **8**, 178-188.

83. Hur,G.M., Ryu,Y.S., Yun,H.Y., Jeon,B.H., Kim,Y.M., Seok,J.H. and Lee,J.H. (1999) Hepatic ischemia/reperfusion in rats induces iNOS gene transcription by activation of NF-kappaB. *Biochem. Biophys. Res. Commun.*, **261**, 917-922.

84. Fan,C., Li,Q., Ross,D. and Engelhardt,J.F. (2003) Tyrosine phosphorylation of I kappa B alpha activates NF kappa B through a redox-regulated and c-Src-dependent mechanism following hypoxia/reoxygenation. *J. Biol. Chem.*, **278**, 2072-2080.

85. He,S.Q., Zhang,Y.H., Venugopal,S.K., Dicus,C.W., Perez,R.V., Ramsamooj,R., Nantz,M.H., Zern,M.A. and Wu,J. (2006) Delivery of antioxidative enzyme genes protects against ischemia/reperfusion-induced liver injury in mice. *Liver Transpl.*, **12**, 1869-1879.

86. Zhong,Z., Froh,M., Connor,H.D., Li,X., Conzelmann,L.O., Mason,R.P., Lemasters,J.J. and Thurman,R.G. (2002) Prevention of hepatic ischemia-reperfusion injury by green tea extract. *Am. J. Physiol Gastrointest. Liver Physiol*, **283**, G957-G964.

87. Matsui,N., Kasajima,K., Hada,M., Nagata,T., Senga,N., Yasui,Y., Fukuishi,N. and Akagi,M. (2005) Inhibiton of NF-kappaB activation during ischemia reduces hepatic ischemia/reperfusion injury in rats. *J. Toxicol. Sci.*, **30**, 103-110.

88. Luedde,T., Assmus,U., Wustefeld,T., Meyer,z., V, Roskams,T., Schmidt-Supprian,M., Rajewsky,K., Brenner,D.A., Manns,M.P., Pasparakis,M. *et al.* (2005) Deletion of IKK2 in hepatocytes does not sensitize these cells to TNF-induced apoptosis but protects from ischemia/reperfusion injury. *J. Clin. Invest*, **115**, 849-859.

89. Takahashi,Y., Ganster,R.W., Ishikawa,T., Okuda,T., Gambotto,A., Shao,L., Murase,N. and Geller,D.A. (2001) Protective role of NF-kappaB in liver cold ischemia/reperfusion injury: effects of IkappaB gene therapy. *Transplant. Proc.*, **33**, 602.

90. Tsung,A., Hoffman,R.A., Izuishi,K., Critchlow,N.D., Nakao,A., Chan,M.H., Lotze,M.T., Geller,D.A. and Billiar,T.R. (2005) Hepatic ischemia/reperfusion injury involves functional TLR4 signaling in nonparenchymal cells. *J. Immunol.*, **175**, 7661-7668.

91. Kuboki,S., Okaya,T., Schuster,R., Blanchard,J., Der,C.J., Denenberg,A., Wong,H. and Lentsch,A.B. (2007) Hepatocyte NF-kappaB activation is hepatoprotective during IRI and is augmented by ischemic hypothermia. *Am. J. Physiol Gastrointest. Liver Physiol*, **292**, G201-G207.

92. Glantzounis,G.K., Salacinski,H.J., Yang,W., Davidson,B.R. and Seifalian,A.M. (2005) The contemporary role of antioxidant therapy in attenuating liver ischemia-reperfusion injury: a review. *Liver Transpl.*, **11**, 1031-1047.

93. Selzner,N., Rudiger,H., Graf,R. and Clavien,P.A. (2003) Protective strategies against ischemic injury of the liver. *Gastroenterology*, **125**, 917-936.

94. Gerwig,T., Meissner,H., Bilzer,M., Kiemer,A.K., Arnholdt,H., Vollmar,A.M. and Gerbes,A.L. (2003) Atrial natriuretic peptide preconditioning protects against hepatic preservation injury by attenuating necrotic and apoptotic cell death. *J. Hepatol.*, **39**, 341-348.

95. Fan,C., Zwacka,R.M. and Engelhardt,J.F. (1999) Therapeutic approaches for ischemia/reperfusion injury in the liver. *J. Mol. Med.*, **77**, 577-592.

96. Koti,R.S., Seifalian,A.M. and Davidson,B.R. (2003) Protection of the liver by ischemic preconditioning: a review of mechanisms and clinical applications. *Dig. Surg.*, **20**, 383-396.

97. Funaki,H., Shimizu,K., Harada,S., Tsuyama,H., Fushida,S., Tani,T. and Miwa,K. (2002) Essential role for nuclear factor kappaB in ischemic preconditioning for ischemia-reperfusion injury of the mouse liver. *Transplantation*, **74**, 551-556.

98. Teoh,N., Dela,P.A. and Farrell,G. (2002) Hepatic ischemic preconditioning in mice is associated with activation of NF-kappaB, p38 kinase, and cell cycle entry. *Hepatology*, **36**, 94-102.

99. Carini,R. and Albano,E. (2003) Recent insights on the mechanisms of liver preconditioning. *Gastroenterology*, **125**, 1480-1491.

100. Teoh,N., Leclercq,I., Pena,A.D. and Farrell,G. (2003) Low-dose TNF-alpha protects against hepatic ischemia-reperfusion injury in mice: implications for preconditioning. *Hepatology*, **37**, 118-128.

101. Kupatt,C., Habazettl,H., Goedecke,A., Wolf,D.A., Zahler,S., Boekstegers,P., Kelly,R.A. and Becker,B.F. (1999) Tumor necrosis factor-alpha contributes to ischemia- and reperfusion-induced endothelial activation in isolated hearts. *Circ. Res.*, **84**, 392-400.

102. Romano,M.F., Lamberti,A., Bisogni,R., Tassone,P., Pagnini,D., Storti,G., Del Vecchio,L., Turco,M.C. and Venuta,S. (2000) Enhancement of cytosine arabinoside-induced apoptosis in human myeloblastic leukemia cells by NF-kappa B/Rel- specific decoy oligodeoxynucleotides. *Gene Ther.*, **7**, 1234-1237.

103. Coester,C. (2003) Development of a new carrier system for oligonucleotides and plasmids based on gelatin nanoparticles. *New Drugs*, **1**, 14-17.

104. Pfaffl,M.W. (2001) A new mathematical model for relative quantification in real-time RT-PCR. *Nucleic Acids Res.*, **29**, e45.

105. Samsom,J.N., Annema,A., Groeneveld,P.H., Van Rooijen,N., Langermans,J.A. and van Furth,R. (1997) Elimination of resident macrophages from the livers and spleens of immune mice impairs acquired resistance against a secondary Listeria monocytogenes infection. *Infect. Immun.*, **65**, 986-993.

106. Pinto,A.J., Stewart,D., Van Rooijen,N. and Morahan,P.S. (1991) Selective depletion of liver and splenic macrophages using liposomes encapsulating the drug dichloromethylene diphosphonate: effects on antimicrobial resistance. *J. Leukoc. Biol.*, **49**, 579-586.

107. Xiong,S., She,H., Sung,C.K. and Tsukamoto,H. (2003) Iron-dependent activation of NF-kappaB in Kupffer cells: a priming mechanism for alcoholic liver disease. *Alcohol*, **30**, 107-113.

108. Kiemer,A.K., Muller,C. and Vollmar,A.M. (2002) Inhibition of LPS-induced nitric oxide and TNF-alpha production by alpha-lipoic acid in rat Kupffer cells and in RAW 264.7 murine macrophages. *Immunol. Cell Biol.*, **80**, 550-557.

109. Tsoulfas,G. and Geller,D.A. (2001) NF-kappaB in transplantation: friend or foe? *Transpl. Infect. Dis.*, **3**, 212-219.

110. Chaisson,M.L., Brooling,J.T., Ladiges,W., Tsai,S. and Fausto,N. (2002) Hepatocyte-specific inhibition of NF-kappaB leads to apoptosis after TNF treatment, but not after partial hepatectomy. *J. Clin. Invest*, **110**, 193-202.

111. Barratt,G. (2003) Colloidal drug carriers: achievements and perspectives. *Cell Mol. Life Sci.*, **60**, 21-37.

112. Daemen,T., Velinova,M., Regts,J., de Jager,M., Kalicharan,R., Donga,J., van der Want,J.J. and Scherphof,G.L. (1997) Different intrahepatic distribution of phosphatidylglycerol and phosphatidylserine liposomes in the rat. *Hepatology*, **26**, 416-423.

113. Higuchi,Y., Kawakami,S., Nishikawa,M., Yamashita,F. and Hashida,M. (2005) Intracellular distribution of NFkappaB decoy and its inhibitory effect on TNFalpha production by LPS stimulated RAW 264.7 cells. *J. Control Release*, **107**, 373-382.

114. Bene,A., Kurten,R.C. and Chambers,T.C. (2004) Subcellular localization as a limiting factor for utilization of decoy oligonucleotides. *Nucleic Acids Res.*, **32**, e142.

115. Griesenbach,U., Cassady,R.L., Cain,R.J., duBois,R.M., Geddes,D.M. and Alton,E.W. (2002) Cytoplasmic deposition of NFkappaB decoy oligonucleotides is insufficient to inhibit bleomycin-induced pulmonary inflammation. *Gene Ther.*, **9**, 1109-1115.

116. Li,Y.Y., Wong,L.Y., Cheung,B.M., Hwang,I.S. and Tang,F. (2005) Differential induction of adrenomedullin, interleukins and tumour necrosis

factor-alpha by lipopolysaccharide in rat tissues in vivo. *Clin. Exp. Pharmacol. Physiol*, **32**, 1110-1118.

117. Bohrer,H., Qiu,F., Zimmermann,T., Zhang,Y., Jllmer,T., Mannel,D., Bottiger,B.W., Stern,D.M., Waldherr,R., Saeger,H.D. *et al.* (1997) Role of NFkappaB in the mortality of sepsis. *J. Clin. Invest*, **100**, 972-985.

118. Luedde,T., Beraza,N. and Trautwein,C. (2006) Evaluation of the role of nuclear factor-kappaB signaling in liver injury using genetic animal models. *J. Gastroenterol. Hepatol.*, **21 Suppl 3**, S43-S46.

119. Kato,A., Edwards,M.J. and Lentsch,A.B. (2002) Gene deletion of NF-kappa B p50 does not alter the hepatic inflammatory response to ischemia/reperfusion. *J. Hepatol.*, **37**, 48-55.

120. DeAngelis,R.A., Kovalovich,K., Cressman,D.E. and Taub,R. (2001) Normal liver regeneration in p50/nuclear factor kappaB1 knockout mice. *Hepatology*, **33**, 915-924.

121. Uesugi,T., Froh,M., Arteel,G.E., Bradford,B.U., Gabele,E., Wheeler,M.D. and Thurman,R.G. (2001) Delivery of IkappaB superrepressor gene with adenovirus reduces early alcohol-induced liver injury in rats. *Hepatology*, **34**, 1149-1157.

122. Lavon,I., Goldberg,I., Amit,S., Landsman,L., Jung,S., Tsuberi,B.Z., Barshack,I., Kopolovic,J., Galun,E., Bujard,H. *et al.* (2000) High susceptibility to bacterial infection, but no liver dysfunction, in mice compromised for hepatocyte NF-kappaB activation. *Nat. Med.*, **6**, 573-577.

123. Gerondakis,S., Grossmann,M., Nakamura,Y., Pohl,T. and Grumont,R. (1999) Genetic approaches in mice to understand Rel/NF-kappaB and IkappaB function: transgenics and knockouts. *Oncogene*, **18**, 6888-6895.

124. Dajani,R., Sanlioglu,S., Zhang,Y., Li,Q., Monick,M.M., Lazartigues,E., Eggleston,T., Davisson,R.L., Hunninghake,G.W. and Engelhardt,J.F. (2007) Pleiotropic functions of TNF-alpha determine distinct IKKbeta-dependent hepatocellular fates in response to LPS. *Am. J. Physiol Gastrointest. Liver Physiol*, **292**, G242-G252.

125. Maeda,S., Kamata,H., Luo,J.L., Leffert,H. and Karin,M. (2005) IKKbeta couples hepatocyte death to cytokine-driven compensatory proliferation that promotes chemical hepatocarcinogenesis. *Cell*, **121**, 977-990.

126. Fernandez,V., Castillo,I., Tapia,G., Romanque,P., Uribe-Echevarria,S., Uribe,M., Cartier-Ugarte,D., Santander,G., Vial,M.T. and Videla,L.A. (2007)

Thyroid hormone preconditioning: protection against ischemia-reperfusion liver injury in the rat. *Hepatology*, **45**, 170-177.

127. Yoshidome,H., Kato,A., Edwards,M.J. and Lentsch,A.B. (1999) Interleukin-10 suppresses hepatic ischemia/reperfusion injury in mice: implications of a central role for nuclear factor kappaB. *Hepatology,* **30**, 203-208.

128. Demirbilek,S., Karaman,A., Gurunluoglu,K., Tas,E., Akin,M., Aksoy,R.T., Turkmen,E., Edali,M.N. and Baykarabulut,A. (2006) Polyenylphosphatidylcholine pretreatment protects rat liver from ischemia/reperfusion injury. *Hepatol. Res.*, **34**, 84-91.

129. Liu,Z.J., Yan,L.N., Li,S.W., You,H.B. and Gong,J.P. (2006) Glycine blunts transplantative liver ischemia-reperfusion injury by downregulating interleukin 1 receptor associated kinase-4. *Acta Pharmacol. Sin.*, **27**, 1479-1486.

130. Arsura,M. and Cavin,L.G. (2005) Nuclear factor-kappaB and liver carcinogenesis. *Cancer Lett.*, **229**, 157-169.

131. Hill,D.B., Devalaraja,R., Joshi-Barve,S., Barve,S. and McClain,C.J. (1999) Antioxidants attenuate nuclear factor-kappa B activation and tumor necrosis factor-alpha production in alcoholic hepatitis patient monocytes and rat Kupffer cells, in vitro. *Clin. Biochem.*, **32**, 563-570.

132. Nakamuta,M., Ohta,S., Tada,S., Tsuruta,S., Sugimoto,R., Kotoh,K., Kato,M., Nakashima,Y., Enjoji,M. and Nawata,H. (2001) Dimethyl sulfoxide inhibits dimethylnitrosamine-induced hepatic fibrosis in rats. *Int. J. Mol. Med.*, **8**, 553-560.

133. Lentsch,A.B. (2005) Activation and function of hepatocyte NF-kappaB in postischemic liver injury. *Hepatology*, **42**, 216-218.

8 APPENDIX

8.1 Abbreviations

ALT	alanine amino transferase
ANP	atrial natriuretic peptide
AP-1	activator protein 1
AST	aspartate amino transferase
BSA	bovine serum albumin
cAMP	cyclic adenosine-5'-monophosphate
CINC	cytokine-induced neutrophil chemoattractant
CLSM	confocal laser scanning microscopy
COX	cyclooxygenase
CREB	cAMP response element-binding protein
DEN	diethylnitrosamine
DMEM	Dulbecco´s modified eagle medium
DNA	desoxyribonucleic acid
DOPC	dioleoyl-glycero-3-phosphocholine
DOTAP	dioleoyl-trimethylammonium-propane
DTT	dithiothreitol
EDC	ethyl-(dimethylaminopropyl)carbodiimide hydrochloride
Egr-1	early growth response factor 1
EMSA	electrophoretic mobility shift assay
eNOS/iNOS	endothelial/inducible NO synthetase
FBS	fetal bovine serum
GAPDH	glyceraldehyde-3-phosphate dehydrogenase

HAT	histone acetyltransferase
HDAC	histone deacetylase
HVJ	hemagglutinating virus of Japan
ICAM	intercellular adhesion molecule
IKK	IκB kinase
IL	interleukin
IP	ischemic preconditioning
IR	ischemia/reperfusion
IRAK	interleukin-1 associated kinase
IκB	inhibitory protein κB
LBP	LPS binding protein
LPS	lipopolysaccharide
MCP	monocyte chemoattractant protein
MIP	macrophage inflammatory protein
mRNA	messenger ribonucleic acid
NAC	N-acetylcysteine
NEMO	nuclear factor κB essential modulator
NF-κB	nuclear factor κB
NP	nanoparticle
NP-40	non-ident P 40
NSAID	non-steroidal anti-inflammatory drugs
ODN	oligodeoxynucleotide
PBS	phosphate buffered saline
PDTC	pyrrolidinedithiocarbamate
PE	polyethylene

PMSF	phenylmethylsulfonylfluoride
PTO	phosphorothioate
ROS	reactive oxygen species
RT-PCR	reverse transcription polymerase chain reaction
TGF	transforming growth factor
TLR	toll-like receptor
TNF-α	tumor necrosis factor-α
TRAF	TNF-receptor associated factor
UW	University of Wisconsin solution

8.2 Alphabetical list of companies

Abbott	Wiesbaden, Germany
Air Liquide	Duesseldorf, Germany
Amersham	Freiburg, Germany
Applied Biosystems	Hamburg, Germany
ATCC	Rockville, USA
Beckman Coulter	Krefeld, Germany
Biomers.net	Ulm, Germany
Biosource	Camarillo, USA
Cambrex Profarmaco	Landen, Belgium
Charles-River Laboratories	Sulzfeld, Germany
GraphPad Software	San Diego, USA
Invitrogen	Karlsruhe, Germany
Janssen-Cilag	Neuss, Germany
Labvision	Fremont, USA
PAA Laboratories	Linz, Austria
Peske	Aindling-Pichl, Germany
Promega	Heidelberg, Germany
Qiagen	Hilden, Germany
Ratiopharm	Ulm, Germany
Roche Diagnostics	Mannheim, Germany
Serotec	Duesseldorf, Germany
Sigma-Aldrich	Taufkirchen, Germany

Ssniff	Soest, Germany
Stratagene	LaJolla, USA
Thermo Shandon	Frankfurt, Germany
USB	Cleveland, USA
VWR	Ismaning, Germany
Zeiss	Jena, Germany

8.3 Publications

8.3.1 Original Publications

Hoffmann F, Zillies J, Zahler S, Coester C, Winter G, Vollmar AM.

NF-κB Decoy Oligonucleotides loaded Gelatin Nanoparticles – a Tool for selective Inhibition of NF-κB in activated Kupffer cells in vivo. *Gene Therapy*. 2007 submitted.

Plesnila N, Baumgarten L, Retiounskaia M, Engel D, Zimmermann R, Hoffmann F, Landshamer S, Culmsee C.

Delayed Neuronal Death after Brain Trauma involves p53-dependent Inhibition of NF-κB Transcriptional Activity. *Cell Death and Differentiation*. 2007 in press.

Zischka H, Larochette N, Hoffmann F, Hamöller D, Jägemann N, Lichtmannegger J, Jennen L, Goettlicher M, Vollmar AM, Kroemer G.

Mitochondria at the point of no return: Differential Analysis of the Permeability Transition by Free Flow Electrophoresis. 2007 in preparation

8.3.2 Oral presentations

Hoffmann F, Zillies J, Zahler S, Coester C, Winter G, Vollmar AM

Targeting NF-κB selectively in Kupffer cells with NF-κB decoy oligodeoxynucleotides is a promising tool for influencing inflammatory liver signalling.

48th Spring Meeting of the Deutsche Gesellschaft für experimentelle und klinische Pharmakologie und Toxikologie, March 13-15, 2007, Mainz, Germany.

Naunyn Schmiedeberg´s Arch Pharmacol. 2007; 375 Suppl1: R51

8.4 Curriculum vitae

Persönliche Daten

Name:	Florian Hoffmann
Geburtstag und −ort:	08. August 1974, München
Staatsangehörigkeiten:	deutsch, österreichisch
Familienstand:	ledig

Promotion

08/2003 – 06/2007	Department of Pharmacy, Center of Drug Research, Pharmaceutical Biology, Prof. Dr. A. M. Vollmar

Hochschule

1994 - 2001	Studium der Pharmazie an der Universität Innsbruck, Österreich
02 – 09/1995	Auslandsstudium an der University of Queensland, Brisbane, Australien
21.10.1997	Erste Diplomprüfung
10/1999 – 03/2000	Diplomarbeit am Institut für Pharmakognosie, Universität Innsbruck, Österreich
18.12.2001	Zweite Diplomprüfung

Schule

1981 – 1994	Grundschule Wörth am Main, Hermann-Staudinger-Gymnasium Erlenbach am Main, Deutschland
	Abschluss: Abitur

Berufsausbildung

02/2002 – 08/2002	Pharmaziepraktikum in der Löwenapotheke, Bamberg, Deutschland
08/2002 – 02/2003	Pharmaziepraktikum bei Dr. Robert Pfleger GmbH, Bamberg, Deutschland

8.5 Acknowledgements